MASTER'S DEGREE THESIS

Master of Science in Advanced Mathematics and Mathematical Engineering

Title: How to Apply Numerical Tools to Study Dynamical Systems: The CP Problem

Author: Montserrat Aranda May

Advisor: Dr. Mercè Ollé

Department: Applied Mathematics I

Academic year: 2013/2014

UNIVERSITAT POLITÈCNICA DE CATALUNYA
BARCELONATECH
Facultat de Matemàtiques i Estadística

How to Apply Numerical Tools to Study Dynamical Systems: The CP Problem

Montserrat Aranda May

UNIVERSITAT POLITÈCNICA
DE CATALUNYA
BARCELONATECH

Advisor:
Dr. Mercè Ollé

This thesis is submitted for the degree of

Master in Advanced Mathematics and Mathematical Engineering

Polytechnic University of Catalonia
Faculty of Mathematics and Statistics
Barcelona

22 June 2014

For all of those who enjoy thinking and reasoning, in other words, for everyone that "does Mathematics"

Contents

1 The CP problem **3**
- 1.1 Equations and basic features of the CP problem . . . 3
  - 1.1.1 Equations of the problem . . . 3
  - 1.1.2 Equilibrium points of the CP problem . . . 6
  - 1.1.3 Linear stability of equilibria . . . 7

2 Computation of $\mathcal{L}_1$ and $\mathcal{L}_2$ **13**

3 Hill's Regions **15**
- 3.1 First approach to Hill's regions . . . 15
- 3.2 Zero Velocity Curves . . . 17
  - 3.2.1 Pseudo-Arc Method . . . 17

4 Homoclinic connections to $\mathcal{L}_1$ **19**
- 4.1 Introduction to the stable and unstable manifolds of the CP problem . . . 20
- 4.2 Symmetric homoclinic connections . . . 22
  - 4.2.1 Inner connections . . . 22
  - 4.2.2 Outer connections . . . 26

5 Variational equations **29**

6 Dynamics from a global point of view **31**
- 6.1 The two-body problem: $K = 0$ . . . 31
  - 6.1.1 Description of the problem . . . 31
  - 6.1.2 Equilibria of the two-body problem . . . 35
  - 6.1.3 Hill's Regions when $K = 0$ . . . 36
  - 6.1.4 Rotating ellipses, parabolas and hyperbolas . . . 38
  - 6.1.5 Poincaré section plots when $K = 0$ . . . 40
- 6.2 Introduction to global dynamics for $K > 0$ . . . 43

7 Periodic orbits **47**
- 7.1 Implementation of PO . . . 50
- 7.2 Continuation of families of PO . . . 53
  - 7.2.1 Family of direct PO . . . 54
  - 7.2.2 Family of internal retrograde PO . . . 55
  - 7.2.3 Family of external retrograde PO . . . 56
  - 7.2.4 Lyapunov periodic orbits . . . 57

7.3 Global dynamics for $K > 0$: coming back to PSP 62

8 Homoclinic connections to LPO **65**
8.1 Invariant manifolds of the LPO around $\mathcal{L}_1$ 66

9 Conclusions **69**

References **70**

Introduction

My interest in Numerical Methods and Dynamical Systems gave me the idea of combining both disciplines and creating the thesis *How to Apply Numerical Tools to Study Dynamical Systems: The CP Problem* as the last step to finish the *Master in Advanced Mathematics and Mathematical Engineering* at the Polytechnic University of Catalonia. During the elaboration of this project I attended to the Master's course *Numerical Methods for Dynamical Systems*, which was structured on the same topic as my project and whose lecturer was Mercè Ollé, also the advisor of my thesis.

Consider a dynamical system modelled using a system of differential equations,

$$\dot{\mathbf{x}} = \mathbf{f}(\mathbf{x}), \tag{1}$$

being $\mathbf{f}$ smooth enough in $\mathcal{U} \subset \mathbb{R}^n$, for $\mathcal{U}$ an open set. Normally it is not possible to find the solutions of (1) analytically, so other ways have to be taken into account in order to describe the behaviour of the system. The goal of my thesis is to study how to construct numerically the skeleton of a given dynamical system, starting with the computation of the easiest solutions -equilibrium points- and following with other invariant objects as manifolds of equilibria, homoclinic orbits, periodic orbits (PO), manifolds of PO, chaos, island chains, etc. Thanks to these particular solutions and using well-known theory of Dynamical Systems, one can get an idea of the general behaviour of system (1).

In order to study how to construct such a skeleton, the project focus its attention on the system that models the behaviour of a hydrogen atom in a circularly polarized microwave field (known as *the CP problem*), following mainly paper [1], where a similar study has been done. Along the project we introduce the necessary knowledge of Dynamical Systems and Hamiltonian Systems to understand the contents of this paper and reproduce correctly its numerical simulations, refering sometimes to [2].

There exist studies based in other problems and similar to the one that is going to be explained, for example [8] shows the case of the RTBP (restricted three-body problem).

During the elaboration of this thesis, several code routines have been implemented to deduce the structure of the solutions of (1). In these routines there appear numerical methods as the *multidimensional Newton's method*, the *bisection method*, the *pseudo-arc method*, among others. The programming language used is C++, with the useful library for linear algebra *Eigen* (see manual [9]). All the computations have been done using double precision. Moreover we have used the *Taylor* ODE integrator, read [5] to learn how it works. Remark that one could choose other types of ODE integrators, like *Runge-Kutta*.

The thesis is organized in eight chapters which are mostly self contained but which complement each other. In the first chapter of the thesis the CP problem is introduced, from the Hamiltonian system of differential equations that models the problem to some important features of it (symmetry, location of equilibria, stability of equilibria, etc.). Actually we obtain a system of ordinary differential equations

that depends only on one parameter K. The deduction of the equations of the problem from a physical point of view is not studied, since our interest is pure mathematician; so for further information about the modellization see [1]. In chapter 2 the position of the equilibrium points of (1) and their energy level when $K > 0$ varies are computed, thanks to the implementation of an unidimensional Newton's method. A numerical study of the Hill's regions of the CP problem when $K > 0$ can be found in chapter 3, starting with a first approach of them and finishing with the computation of the zero velocity curves (zvc), which are the boundary of the commented regions. In chapter 4 the invariant manifolds of unstable equilibria are considered, and we also analyze the existence of symmetric homoclinic connections to the equilibrium point. Such homoclinic connections allow us to obtain a first idea of the local (and also global) behaviour around an equilibrium point with hyperbolic part. Chapter 5 is a fast review of Variational equations. Then, in chapter 6 we present a detailed description of the main features of the dynamics from a global point of view for $K = 0$ and $K = 0.0015749$ (of course other values of $K > 0$ small can be considered). Suitable Poincaré sections are taken and the evolution of the different objects involved in the dynamics are described, when the parameter changes from 0 to 0.0015749. In the same chapter it is shown that, when the parameter of the CP problem is 0, we are in front of the two-body problem. In chapter 7 we give a description of the main families of periodic orbits of the problem by using global results from chapter 6 and the well-known *Lyapunov center theorem*. Thanks to our implementation, we do the continuation of these families of PO when varying the energy level. Finally, in chapter 8 a basic study of the invariant manifolds of hyperbolic Lyapunov periodic orbits (LPO) around the equilibrium point is exposed, talking also a little about the existence of homoclinic connections to the LPO. Conclusions are in chapter 9.

Finally, I would like to thank my thesis advisor, Mercè Ollé. At several points during my thesis work, her help, patience and motivation encouraged me to learn always a little bit more.

1 The CP problem

We consider the problem of a hydrogen atom interacting with a circularly polarized (CP) microwave field. This problem can be modeled as a perturbed Kepler problem, and in particular we are interested in the possible motions of the electron assuming a proton in the nucleus.

The Hamiltonian for a hydrogen atom (in atomic units and in the limit of an infinitely massive nucleus) subjected to a CP microwave field is the following:

$$\mathcal{H} = \frac{1}{2}(p_x^2 + p_y^2 + p_z^2) - \frac{1}{r} + F(x\cos\omega t + y\sin\omega t), \tag{1.1}$$

where (x, y, z) and (p_x, p_y, p_z) are the canonical coordinates and their conjugate momenta; $r^2 = x^2 + y^2 + z^2$; ω is the angular frequency of the microwave field and $F > 0$ is the field strength. We are going to study the motion in the planar case, that is for $z = 0$, so we omit the variables z and p_z.

1.1 Equations and basic features of the CP problem

In this section, we are going to study the equations of the problem, giving then some basic properties of it.

1.1.1 Equations of the problem

Considering the Hamiltonian given by (1.1) and moving to a frame rotating with the CP field (with angular velocity ω), the Hamiltonian becomes autonomous and its expression is

$$\mathcal{H}_1 = \frac{1}{2}(p_x^2 + p_y^2) - \omega(xp_y - yp_x) - \frac{1}{r} + Fx, \tag{1.2}$$

where now (x, y) and (p_x, p_y) correspond to positions and momenta in the rotating frame. This Hamiltonian can be simplified by re-scaling time and distances:

- Define a new time $s = \omega t$.
- Introduce the symplectic change of coordinates with multiplier $a^2\omega$,

$$(x, y) = a(\bar{x}, \bar{y}) \quad (p_x, p_y) = a\omega(\bar{p_x}, \bar{p_y}). \tag{1.3}$$

1.1.1 Remark Remember the following:

- If you scale time by $t \to \omega t$, then you should scale the Hamiltonian by $\mathcal{H}_1 \to \mathcal{H}_1 \frac{1}{\omega}$.
- A change of variables is symplectic with multiplier μ if and only if its differential matrix D satisfies $DJD^T = \mu J$ at each point (x, y, p_x, p_y) of the domain.

  In our case,

$$D = \begin{pmatrix} a & 0 & 0 & 0 \\ 0 & a & 0 & 0 \\ 0 & 0 & a\omega & 0 \\ 0 & 0 & 0 & a\omega \end{pmatrix}, \quad D^T = \begin{pmatrix} a & 0 & 0 & 0 \\ 0 & a & 0 & 0 \\ 0 & 0 & a\omega & 0 \\ 0 & 0 & 0 & a\omega \end{pmatrix}, \quad J = \begin{pmatrix} 0 & 0 & 1 & 0 \\ 0 & 0 & 0 & 1 \\ -1 & 0 & 0 & 0 \\ 0 & -1 & 0 & 0 \end{pmatrix}$$

  and,

$$\begin{aligned} DJD^T &= \begin{pmatrix} a & 0 & 0 & 0 \\ 0 & a & 0 & 0 \\ 0 & 0 & a\omega & 0 \\ 0 & 0 & 0 & a\omega \end{pmatrix} \begin{pmatrix} 0 & 0 & 1 & 0 \\ 0 & 0 & 0 & 1 \\ -1 & 0 & 0 & 0 \\ 0 & -1 & 0 & 0 \end{pmatrix} \begin{pmatrix} a & 0 & 0 & 0 \\ 0 & a & 0 & 0 \\ 0 & 0 & a\omega & 0 \\ 0 & 0 & 0 & a\omega \end{pmatrix} \\ &= \begin{pmatrix} 0 & 0 & a & 0 \\ 0 & 0 & 0 & a \\ -a\omega & 0 & 0 & 0 \\ 0 & -a\omega & 0 & 0 \end{pmatrix} \begin{pmatrix} a & 0 & 0 & 0 \\ 0 & a & 0 & 0 \\ 0 & 0 & a\omega & 0 \\ 0 & 0 & 0 & a\omega \end{pmatrix} \\ &= \begin{pmatrix} 0 & 0 & a^2\omega & 0 \\ 0 & 0 & 0 & a^2\omega \\ -a^2\omega & 0 & 0 & 0 \\ 0 & -a^2\omega & 0 & 0 \end{pmatrix} \\ &= a^2\omega \begin{pmatrix} 0 & 0 & 1 & 0 \\ 0 & 0 & 0 & 1 \\ -1 & 0 & 0 & 0 \\ 0 & -1 & 0 & 0 \end{pmatrix} = a^2\omega J, \end{aligned}$$

  so (1.3) is a symplectic change of variables with multiplier $a^2\omega$.

See chapter 6 of reference [2] for more information.

The expression of the Hamiltonian (1.2) in the new variables, after dropping the bar of the variables, becomes

$$\mathcal{H}_2 = \left(\frac{1}{2}a^2\omega^2(p_x^2 + p_y^2) - a^2\omega^2(xp_y - yp_x) - \frac{1}{ar} + Fax\right)\frac{1}{a^2\omega}\frac{1}{\omega} \tag{1.4}$$

$$= \left(\frac{1}{2}\omega^{\frac{2}{3}}(p_x^2 + p_y^2) - \omega^{\frac{2}{3}}(xp_y - yp_x) - \frac{\omega^{\frac{2}{3}}}{r} + \frac{Fx}{\omega^{\frac{2}{3}}}\right)\frac{1}{\omega^{\frac{2}{3}}} \tag{1.5}$$

$$= \frac{1}{2}(p_x^2 + p_y^2) - (xp_y - yp_x) - \frac{1}{r} + \frac{Fx}{\omega^{\frac{4}{3}}} \tag{1.6}$$

$$= \frac{1}{2}(p_x^2 + p_y^2) - xp_y + yp_x - \frac{1}{r} + Kx, \tag{1.7}$$

where in (1.4) the multiplier $a^2\omega$ of (1.3) and $ds = \omega dt$ have been used, in (1.5) a has been chosen in such a way that $a^3\omega^2 = 1$ (or, equivalently, $a = \omega^{-\frac{2}{3}}$) and in (1.7) $K = \frac{F}{\omega^{\frac{4}{3}}} > 0$ has been defined. Clearly, the change performed does not have sense if $\omega = 0$.

1.1.2 Remark For $K = 0$, $\mathcal{H}_2$ corresponds to the Hamiltonian of the two-body problem. See chapter 6.

$\mathcal{H}_2$ is the Hamiltonian of the CP problem, which, for simplicity, is called $\mathcal{H}$. Then, the equations of the CP problem are

$$x' = \frac{\partial \mathcal{H}}{\partial p_x} = p_x + y, \tag{1.8}$$

$$y' = \frac{\partial \mathcal{H}}{\partial p_y} = p_y - x, \tag{1.9}$$

$$p_x' = -\frac{\partial \mathcal{H}}{\partial x} = p_y - \frac{x}{r^3} - K, \tag{1.10}$$

$$p_y' = -\frac{\partial \mathcal{H}}{\partial y} = -p_x - \frac{y}{r^3}. \tag{1.11}$$

1.1.3 Lemma *The equations of motion of the CP problem (1.8)-(1.11) satisfy the symmetry*

$$(t, x, y, p_x, p_y) \longrightarrow (-t, x, -y, -p_x, p_y).$$

Proof: Consider the new variables $T = -t$, $X = x$, $Y = -y$, $P_x = -p_x$ and $P_y = p_y$. Note that $r = \sqrt{x^2 + y^2} = \sqrt{X^2 + Y^2}$.

Let us see that $(X(T), Y(T), P_x(T), P_y(T))$ verifies equations (1.8)-(1.11).

$$\begin{aligned}
\frac{dX}{dT} &= \frac{dX}{dt}(-1) \overset{X=x}{=} -\frac{dx}{dt} \overset{(1.8)}{=} -(p_x + y) = -p_x - y = P_x + Y \\
\frac{dY}{dT} &= \frac{dY}{dt}(-1) \overset{Y=-y}{=} -\frac{dy}{dt}(-1) = \frac{dy}{dt} \overset{(1.9)}{=} p_y - x = P_y - X \\
\frac{dP_x}{dT} &= \frac{dP_x}{dt}(-1) \overset{P_x=-p_x}{=} -\frac{dp_x}{dt}(-1) = \frac{dp_x}{dt} \overset{(1.10)}{=} p_y - \frac{x}{r^3} - K = P_y - \frac{X}{r^3} - K \\
\frac{dP_y}{dT} &= \frac{dP_y}{dt}(-1) \overset{P_y=p_y}{=} -\frac{dp_y}{dt} \overset{(1.11)}{=} p_x + \frac{y}{r^3} = -P_x - \frac{Y}{r^3}
\end{aligned}$$

As $(X(T), Y(T), P_x(T), P_y(T))$ is a solution of our system, at time $-T$ it reaches the point

$$(X(-T), Y(-T), P_x(-T), P_y(-T)) = (x(t), -y(t), -p_x(t), p_y(t)).$$

Consequently, if a solution is at (x, y, p_x, p_y) at time t, there exists another solution which is at $(x, -y, -p_x, p_y)$ at time $-t$. □

1.1.4 Remark The above lemma will be very useful during this project. It implies that, for each solution of the equations of motion, there also exists another one which is symmetric with respect to $y = 0$ in the configuration space. In particular, periodic symmetric solutions with respect to $y = 0$ intersect this axis perpendicularly twice. This property could be used to find families of periodic symmetric solutions, but actually we have chosen an alternative method in order to obtain symmetric and non-symmetric periodic orbits (see chapter 7). However the commented symmetry has been used in the study of symmetric homoclinic connections with respect $y = 0$, which can be seen as periodic orbits of infinite period (see chapter 4).

1.1.2 Equilibrium points of the CP problem

We know that the equilibrium points of (1.8)-(1.11) are the solutions of the system

$$p_x + y = 0, \tag{1.12}$$
$$p_y - x = 0, \tag{1.13}$$
$$p_y - \frac{x}{r^3} - K = 0, \tag{1.14}$$
$$-p_x - \frac{y}{r^3} = 0. \tag{1.15}$$

By using (1.12), we obtain $y = -p_x$, and replacing it in (1.15) the following equation is obtained

$$y - \frac{y}{r^3} = 0. \tag{1.16}$$

By using (1.13), we obtain $x = p_y$, and replacing it in (1.14) the following equation is obtained

$$x - \frac{x}{r^3} - K = 0. \tag{1.17}$$

So, the equilibrium points of the CP problem can be found as the solutions of (1.16)-(1.17). Observe that (1.16) can be rewritten as $y\left(1 - \frac{1}{r^3}\right) = 0$, so (1.16) is satisfied only when $y = 0$ or $r = 1$. Substituting $r = 1$ in (1.17) we have $K = 0$, which corresponds to the two body problem. Restricting our attention only to $K > 0$, then $y = 0$ and the x-coordinate of an equilibrium point has to satisfy

$$x - \frac{x}{|x|^3} - K = 0 \Leftrightarrow \begin{cases} x - \frac{x}{x^3} - K = 0 \Leftrightarrow x^3 - Kx^2 - 1 = 0 & \text{if } x > 0, \\ x - \frac{x}{-(x^3)} - K = 0 \Leftrightarrow x^3 - Kx^2 + 1 = 0 & \text{if } x < 0, \end{cases}$$

or, equivalently,

$$f(x) = x^3 - Kx^2 - sign(x) = 0, \tag{1.18}$$

which has been deduced from (1.17) using the fact that the y-coordinate of an equilibrium point is 0 and, consequently, $r = \sqrt{x^2} = |x|$.

The following lemma talks about the number of equilibrium points of our system and their location.

1.1.5 Lemma *The problem given by the equations of motion (1.8)-(1.11) has only two equilibrium points located at $(x_i, 0)$, $i = 1, 2$, with the following properties:*

1) $\max\left(-1, \frac{-1}{\sqrt{K}}\right) < x_1 < 0$ *and* $x_2 > \max\left(1, \frac{2K}{3}\right)$*;*

2) $\lim_{K\to 0} x_1 = -1$ *and* $\lim_{K\to 0} x_2 = 1$*;*

3) both x_i, $i = 1, 2$, are increasing functions of K.

Proof: Observe that $f'(x) = 3x^2 - 2Kx = x(3x - 2K)$. If $x < 0$, $f'(x) > 0$. If $x > 0$, $f'(x) > 0$ if and only if $x > \frac{2K}{3}$, and $f'(x) < 0$ if and only if $x \in \left(0, \frac{2K}{3}\right)$.

1) On one side, the function $f(x)$ defined in (1.18), increases in $(-\infty, 0)$, $f(-1) = -K < 0$, $f\left(\frac{-1}{\sqrt{K}}\right) = \frac{-1}{\sqrt{K^3}} < 0$ and $\lim_{x\to 0^-} f(x) = 1$. On the other side, the function $f(x)$ decreases over $\left(0, \frac{2K}{3}\right)$, increases in $\left(\frac{2K}{3}, +\infty\right)$, $f(1) = -K < 0$, $f\left(\frac{2K}{3}\right) < 0$, $\lim_{x\to 0^+} f(x) = -1$ and $\lim_{x\to\infty} f(x) = \infty$. Thus, using Bolzano's theorem and the qualitative behaviour of function f, there only exist two solutions of $f(x) = 0$, $x_1 < 0 < x_2$, satisfying the properties of the first statement.

2) Second statement comes directly from the continuity of x_i, $i = 1, 2$, with respect K. In case of x_1, observe that $\lim_{K\to 0} \max\left(-1, \frac{-1}{\sqrt{K}}\right) = -1$ and $\lim_{K\to 0} f(-1) = 0$, so $\lim_{K\to 0} x_1 = -1$. In case of x_2, $\lim_{K\to 0} \max\left(1, \frac{2K}{3}\right) = 1$ and $\lim_{K\to 0} f(1) = 0$, so $\lim_{K\to 0} x_2 = 1$.

3) Finally, for each $i = 1, 2$, deriving implicitly the equation $f(x_i) = 0$ with respect to K, we obtain

$$3x_i^2 \frac{\partial x_i}{\partial K} - x_i^2 - 2Kx_i \frac{\partial x_i}{\partial K} = 0,$$

and, reordering some terms, the last expression becomes

$$\frac{\partial x_i}{\partial K}(3x_i^2 - 2Kx_i) = x_i^2.$$

As $x_i^2 > 0$ and, thanks to 1), $x_1 < 0$ and $x_2 > 0$, for any $i = 1, 2$, $3x_i^2 - 2Kx_i = x_i(3x_i - 2K) > 0$, so it is deduced that

$$\frac{\partial x_i}{\partial K} > 0,$$

which implies that x_i is an increasing function of K.

□

We call $\mathcal{L}_i$ the equilibrium point located at $(x_i, 0)$, $i = 1, 2$, and we denote by $h_i = \mathcal{H}(\mathcal{L}_i)$, $i = 1, 2$, the energy at each equilibrium point.

1.1.3 Linear stability of equilibria

In this section we want to study the linear stability of each equilibrium point of the CP problem. First of all we would like to introduce some previous results about stability of solutions in autonomous systems of ODE.

Theory of stability (I)

Consider an autonomous system of ODE

$$\dot{\mathbf{x}} = \mathbf{f}(\mathbf{x}), \tag{1.19}$$

being $\mathbf{f}$ smooth enough in $\mathcal{U} \subset \mathbb{R}^n$, for $\mathcal{U}$ an open set.

1.1.6 Definition $\phi_t(\mathbf{x}) = \phi(t; \mathbf{x})$ is the solution of (1.19) such that

$$\phi_{t_0}(\mathbf{x}) = \mathbf{x}.$$

1.1.7 Definition A solution $\phi(t; \mathbf{x_0})$ can be classified as:

1) *Lyapunov stable* (or *stable*): if $\forall \varepsilon > 0$, $\exists \delta > 0$ such that any solution $\phi(t; \mathbf{x_1})$ with $||\mathbf{x_1} - \mathbf{x_0}|| < \delta$, satisfies $||\phi(t; \mathbf{x_0}) - \phi(t; \mathbf{x_1})|| < \varepsilon$ $\forall t \geq t_0$.

2) *Asymptotically stable*: if it is stable and satisfies

$$\lim_{t\to+\infty} ||\phi(t; \mathbf{x_0}) - \phi(t; \mathbf{x_1})|| = 0.$$

3) *Unstable*: if it is not stable.

1.1.8 Remark An equilibrium point $\mathbf{p}$ of (1.19) can be seen as a constant solution $\phi(t;\mathbf{p}) = \mathbf{p}\ \forall t$. For this reason, given an equilibrium point $\mathbf{p}$, we are interested in its stability.

From now on we will focus on characterizing the equilibrium points of (1.19). Let $\mathbf{A} := \mathbf{Df}(\mathbf{p})$.

1.1.9 Definition If there is no eigenvalue of $\mathbf{A}$ with zero real part, then p (or $\mathbf{A}$) is *hyperbolic*.

1.1.10 Definition If all the eigenvalues are purely imaginary and its Jordan matrix is diagonal, then $\mathbf{p}$ (or $\mathbf{A}$) is *elliptic*.

In the following figure one can see how the behaviour is, in a linear 2-dimensional case, around an equilibrium point depending on its characterization.

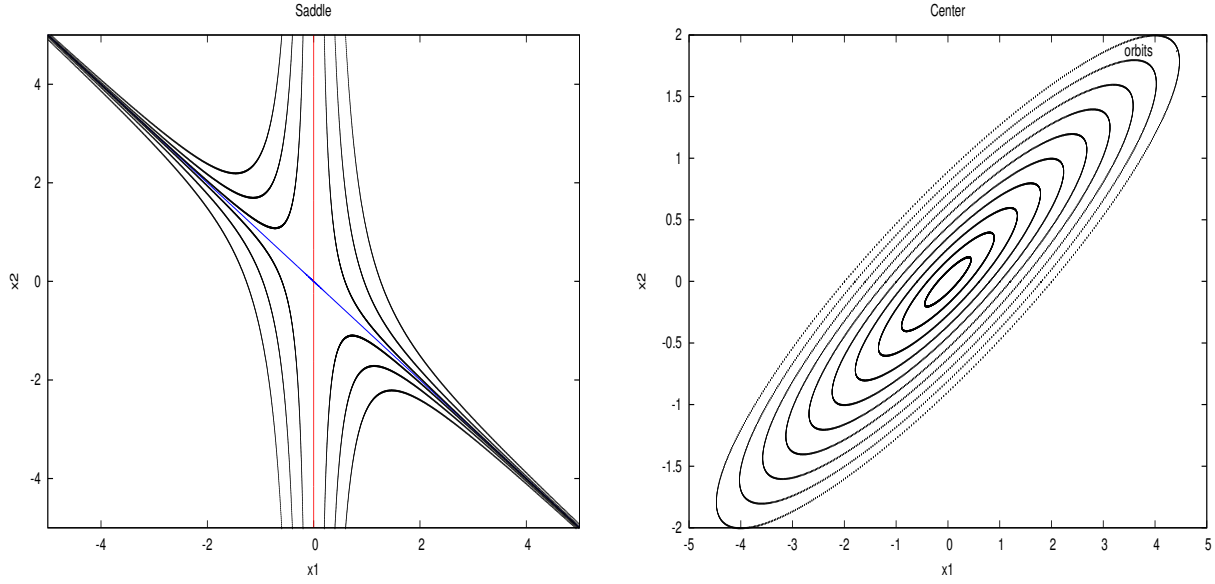

Figure 1.1: Left hand side: $\mathbf{p}$ hyperbolic equilibrium point. Right hand side: $\mathbf{p}$ elliptic equilibrium point.

1.1.11 Remark Thanks to Figure 1.1 we get an idea of the dynamics around the equilibrium point and observe that, in general, in a linear system, hyperbolic equilibria are unstable points, while the elliptic ones are stable.

1.1.12 Theorem ***(Stability of equilibrium points in linear autonomous systems)***

Let us consider $\dot{\mathbf{x}} = \mathbf{A}(\mathbf{x} - \mathbf{p})$, *being* $\mathbf{A}$ *of dimension* $n \times n$ *and* $\mathbf{p}$ *the equilibrium point of the linear system. Then,*

1) If all the eigenvalues satisfy $\Re(\lambda) < 0$, *then* $\mathbf{p}$ *is asymptotically stable.*

2) If there exist eigenvalues with $\Re(\lambda) = 0$ *and they are semisimple (i.e. the corresponding Jordan block is diagonal), and the remaining eigenvalues satisfy* $\Re(\lambda) < 0$, *then* $\mathbf{p}$ *is stable.*

3) In any other situation $\mathbf{p}$ *is unstable.*

Our principal goal now is to study what can be said in the case of non-linear ODE, which is the case of the CP problem.

1.1.13 Theorem ***(Stability of equilibria in non-linear autonomous systems)***

Consider the non-linear autonomous system (1.19) and let $\mathbf{p}$ *be an equilibrium point. If* $\mathbf{p}$ *is hyperbolic, then* $\mathbf{p}$ *is unstable or asymptotically stable. In particular,*

1) If all the eigenvalues of $\mathbf{A}$ *satisfy* $\Re(\lambda) < 0$*, then* $\mathbf{p}$ *is asymptotically stable for (1.19).*

2) If there exists an eigenvalue of $\mathbf{A}$ *such that* $\Re(\lambda) > 0$*, then* $\mathbf{p}$ *is unstable for (1.19).*

We can not say anything about the stability in non-linear systems when $\mathbf{A}$ has all the eigenvalues with zero real part. Then, it is important to recall that we are going to talk about linear stability, and when we write 'stable' it means 'linearly stable'. For additional information about stability see [6] and [7].

1.1.14 Lemma *Suppose that the differential system (1.19) is associated to a Hamiltonian* $\mathcal{H}$ *defined in* $\mathcal{U}$*. Let* $\mathbf{p}$ *be an equilibrium point of the system. If* λ *is an eigenvalue of* $\mathbf{A}$*, then* $-\lambda$*,* $\bar{\lambda}$*,* $-\bar{\lambda}$ *are also eigenvalues of* $\mathbf{A}$

Proof: See [2] for more details.

1.1.15 Remark The last lemma says that the eigenvalues of $\mathbf{A}$ are given in quaterns.

Thanks to this theory, now we are ready to study the stability of $\mathcal{L}_1$ and $\mathcal{L}_2$ taking into account the value of K.

1.1.16 Lemma *Let* $\mathcal{L}_1$*,* $\mathcal{L}_2$ *be the equilibrium points of the problem given by the Hamiltonian (1.7). Then, for* $K > 0$

1) $\mathcal{L}_1$ *is of type center* $\times$ *saddle for all values of* K*.*

2) $\mathcal{L}_2$ *is of type center* $\times$ *center for* $K \leq \frac{3^{-4/3}}{2} \simeq 0.11556021$ *and is a complex saddle for* $K > \frac{3^{-4/3}}{2}$*.*

Proof: Observe that

$$\mathbf{Df}(x, y, p_x, p_y) = \begin{pmatrix} 0 & 1 & 1 & 0 \\ -1 & 0 & 0 & 1 \\ \frac{2x^2-y^2}{r^5} & \frac{3xy}{r^5} & 0 & 1 \\ \frac{3xy}{r^5} & \frac{2y^2-x^2}{r^5} & -1 & 0 \end{pmatrix},$$

and, as the equilibria of our problem are $(x_i, 0, 0, x_i)$, for $i = 1, 2$, we must study the following matrix

$$\mathbf{Df}(x_i, 0, 0, x_i) = \begin{pmatrix} 0 & 1 & 1 & 0 \\ -1 & 0 & 0 & 1 \\ \frac{2}{|x|^3} & 0 & 0 & 1 \\ 0 & \frac{-1}{|x|^3} & -1 & 0 \end{pmatrix}.$$

In order to obtain the eigenvalues of $\mathbf{Df}(x_i, 0, 0, x_i)$, we compute the following determinant,

$$\begin{vmatrix} -\lambda & 1 & 1 & 0 \\ -1 & -\lambda & 0 & 1 \\ \frac{2}{|x_i|^3} & 0 & -\lambda & 1 \\ 0 & \frac{-1}{|x_i|^3} & -1 & -\lambda \end{vmatrix} = \lambda^4 + \left(-\frac{1}{|x_i|^3} + 2\right)\lambda^2 + \frac{1}{|x_i|^3}\left(1 + |x_i|^3 - \frac{2}{|x_i|^3}\right), \tag{1.20}$$

and, by solving

$$\begin{aligned} \lambda^4 + \left(-\frac{1}{|x_i|^3} + 2\right)\lambda^2 + \frac{1}{|x_i|^3}\left(1 + |x_i|^3 - \frac{2}{|x_i|^3}\right) = 0 \quad \Leftrightarrow \\ |x_i|^3\lambda^4 + (-1 + 2|x_i|^3)\lambda^2 + \left(1 + |x_i|^3 - \frac{2}{|x_i|^3}\right) = 0, \end{aligned} \tag{1.21}$$

we obtain the desired eigenvalues:

1) $i = 1$: As $|x_1| = -x_1$, (1.21) becomes

$$-x_1^3\lambda^4 + (-1 - 2x_1^3)\lambda^2 + \left(1 - x_1^3 + \frac{2}{x_1^3}\right),$$

which has roots $\pm\lambda_i$, $i = 1, 2$, where

$$\lambda_1^2 = \frac{1 + 2x_1^3 + \sqrt{8x_1^3 + 9}}{2|x_1|^3},\ \lambda_2^2 = \frac{1 + 2x_1^3 - \sqrt{8x_1^3 + 9}}{2|x_1|^3}.$$

As $-1 < x_1 < 0$, we have

$$\begin{aligned} -3 < -\sqrt{8x_1^3 + 9} < -1, \\ -1 < 1 + 2x_1^3 < 1, \end{aligned}$$

so

$$-\sqrt{8x_1^3 + 9} < 1 + 2x_1^3,$$

which implies $\lambda_1^2 > 0$ for all values of K. In the same way, we have

$$\begin{aligned} 1 < \sqrt{8x_1^3 + 9} < 3, \\ -1 < 1 + 2x_1^3 < 1, \end{aligned}$$

so

$$1 + 2x_1^3 < \sqrt{8x_1^3 + 9},$$

which implies $\lambda_2^2 < 0$ for all values of K. Thanks to these results, we know that the eigenvalues associated to $\mathcal{L}_1$ are of the form: $\pm a$, $\pm bi$, with $a, b \neq 0$, so that $\mathcal{L}_1$ is of type center $\times$ saddle.

2) $i = 2$: As $|x_2| = x_2$, (1.21) becomes

$$x_2^3\lambda^4 + (-1 + 2x_2^3)\lambda^2 + \left(1 + x_2^3 - \frac{2}{x_2^3}\right),$$

which has roots $\pm\lambda_i$, $i = 1, 2$, where

$$\lambda_1^2 = \frac{1 - 2x_2^3 + \sqrt{9 - 8x_2^3}}{2x_2^3},\ \lambda_2^2 = \frac{1 - 2x_2^3 - \sqrt{9 - 8x_2^3}}{2x_2^3}.$$

Observe that the discriminant $9 - 8x_2^3$ is negative if and only if $x_2 > \frac{\sqrt[3]{9}}{2} \simeq 1.0400419$. As we already know, x_2 is the unique positive root of

$$f_+(x) = x^3 - Kx^2 - 1 = 0,$$

and, as $f_+(0) < 0$, $x_2 > 1.0400419$ if and only if

$$f_+(1.0400419) = (1.0400419)^3 - K(1.0400419)^2 - 1 < 0,$$

which means $K > 0.11556021$. Therefore, for $K > 0.11556021$ the discriminant $9 - 8x_2^3 < 0$ and, consequently, $\mathcal{L}_2$ is a complex saddle.

For $K \leq 0.11556021$ the discriminant is positive and, in the same way as we did in 1), both λ_1^2, $\lambda_2^2 < 0$, so the eigenvalues of the equilibrium are of the form: $\pm ai$, $\pm bi$, with $a, b \neq 0$, and, consequently, $\mathcal{L}_2$ is of type center $\times$ center.

□

1.1.17 Remark Observe that, for any positive K, $\mathcal{L}_1$ is an unstable equilibrium, as theorem (1.1.13) states. About the stability of the other equilibrium, $\mathcal{L}_2$, we can say that it is linearly stable for $K \leq \frac{3^{-4/3}}{2}$.

It is important to have this classification in mind in order to understand future procedures.

2 Computation of $\mathcal{L}_1$ and $\mathcal{L}_2$

In this chapter we are interested in knowing the exact position $(x_i, 0)$, $i = 1, 2$, of the two equilibrium points of (1.8)-(1.11) when varying K. In order to do it, we are going to compute x_1 and x_2 ($x_1 < 0 < x_2$) such that $f(x_i) = x_i^3 - Kx_i^2 - sign(x_i) = 0$, $i = 1, 2$, using the results given by lemma (1.1.5).

The main idea of this task is to implement the well-known Newton's method for an unidimensional case. The general structure of the method is, given a seed $x^{(0)}$ close enough to the exact root x of a known function f, better approximations of the root are computed using the recurrence

$$x^{(m+1)} = x^{(m)} - \frac{f(x^{(m)})}{f'(x^{(m)})}, \ m \geq 0, \tag{2.1}$$

until $|f(x^{(m)})| < 10^{-14}$.

On the one side, if we want to obtain the exact value of x_1 we will apply Newton's method to the unidimensional function $f(x_1) = x_1^3 - Kx_1^2 + 1$ with seed $x_1^{(0)} = \max\left(-1, \frac{-1}{\sqrt{K}}\right)$. On the other side, if we want to obtain the exact value of x_2 we will apply Newton's method to the unidimensional function $f(x_2) = x_2^3 - Kx_2^2 - 1$ with seed $x_2^{(0)} = \max\left(1, \frac{2K}{3}\right)$. In both cases the convergence of Newton's method is very fast, only four or five iterations of (2.1) are needed.

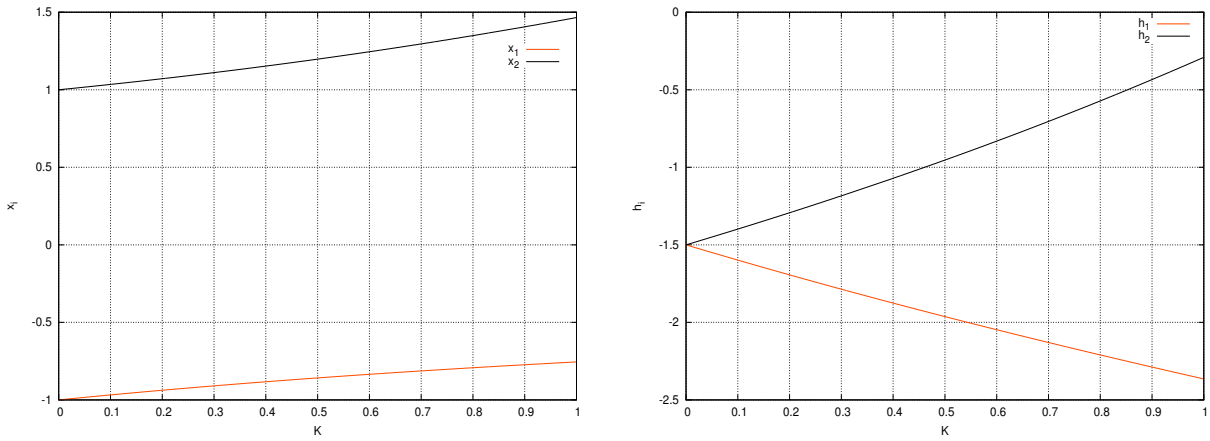

Figure 2.1: Position of the equilibrium points (x-coordinate) and energy of equilibria for $K \in (0, 1)$, respectively.

K	$\mathcal{L}_1$	$\mathcal{L}_2$
0.0015749	$x_1 = -0.99947531$ $h_1 = -1.50157449$	$x_2 = 1.00052524$ $h_2 = -1.49842469$
0.02855986	$x_1 = -0.99057009$ $h_1 = -1.52842477$	$x_2 = 1.00961115$ $h_2 = -1.47130332$
0.03944616	$x_1 = -0.987022650$ $h_1 = -1.53918909$	$x_2 = 1.01332312$ $h_2 = -1.46029220$
0.1	$x_1 = -0.96775311$ $h_1 = -1.59836975$	$x_1 = 1.03446911$ $h_2 = -1.39829568$

Table 2.1: Equilibrium points: position (x-coordinate) and energy for four different values of K.

2.0.18 Remark There exists another possible way to calculate the equilibrium points of our problem: solving directly the cubic equations $f(x_1) = 0$ and $f(x_2) = 0$ by using the corresponding formulas.

In Table 2.1, the position and energy of the equilibrium points for different values of the parameter K are shown (the ones mainly used through the thesis). Through the exposed table, one can check some of the results given in lemma (1.1.5):

- When K goes to $+\infty$, x_1 goes to 0 and x_2 goes to $+\infty$.
- When K tends to 0, x_1 tends to -1 and x_2 tends to 1.
- When K increases, x_1 and x_2 also increase.

3
Hill's Regions

Considering the CP problem, we are interested in knowing, given a value of the parameter $K > 0$, the possible regions of motion, i.e. all the points (x, y) in $\mathbb{R}^2$ that can be reached.

From the expression of the Hamiltonian $\mathcal{H}$, we have

$$\frac{1}{2}(p_x^2 + p_y^2) - xp_y + yp_x - \frac{1}{r} + Kx = h, \tag{3.1}$$

where h is a fixed value of the energy level. As

$$\begin{aligned} x'^2 &= p_x^2 + 2p_x y + y^2, \\ y'^2 &= p_y^2 - 2p_y x + x^2, \end{aligned}$$

then

$$\frac{1}{2}(x'^2 + y'^2) = \frac{p_x^2}{2} + \frac{y^2}{2} + p_x y + \frac{p_y^2}{2} + \frac{x^2}{2} - p_y x,$$

and, as a consequence, (3.1) becomes

$$\frac{1}{2}(x'^2 + y'^2) - \frac{y^2}{2} - \frac{x^2}{2} - \frac{1}{r} + Kx = h. \tag{3.2}$$

Using (3.2),

$$0 \leq \frac{1}{2}(x'^2 + y'^2) = h + \frac{y^2}{2} + \frac{x^2}{2} + \frac{1}{r} - Kx, \tag{3.3}$$

so, only points (x, y) such that

$$h + \frac{y^2}{2} + \frac{x^2}{2} + \frac{1}{r} - Kx \geq 0 \tag{3.4}$$

will be possible. The regions of $\mathbb{R}^2$ where the movement is possible are called *Hill's regions*.

The principal goal of this chapter is to study, for each value h of the energy level, the shape of these regions and how they change when h varies.

3.1 First approach to Hill's regions

In order to get a first idea of the shape of Hill's regions and to know how many components has the region of motion, we take a mesh in the window $[-2, 2] \times [-2, 2]$ and, at each point, the sign of

$$h + \frac{y^2}{2} + \frac{x^2}{2} + \frac{1}{r} - Kx$$

is studied. Then, we take two different colours, one to plot all the points with positive sign, and the other one for the points with negative sign.

After using these method several times we realise that there are only four topologically different cases.

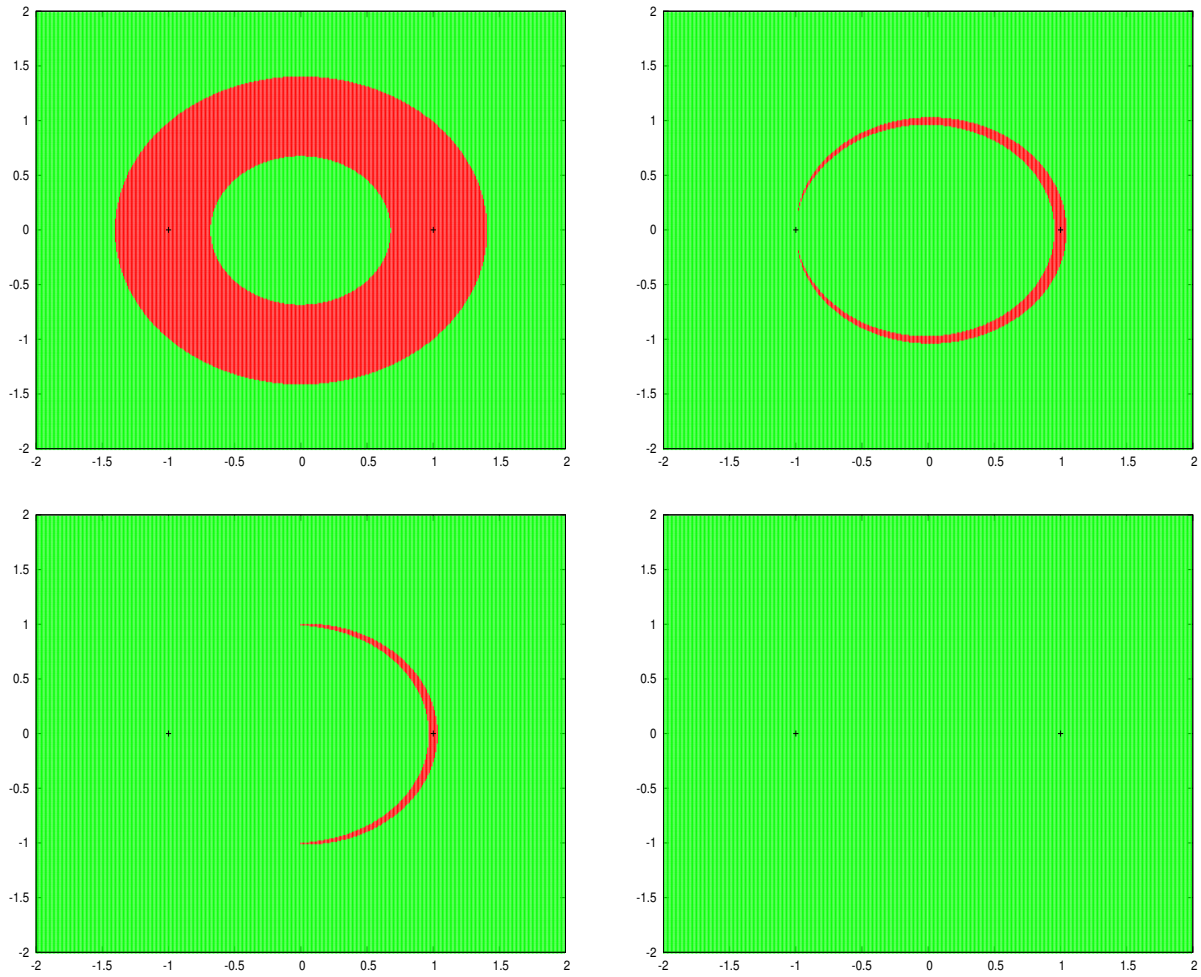

Figure 3.1: Hill's regions in (x, y) coordinates of the CP problem for $K = 0.0015749$ and the following energies: $h = -1.7$ (left, first row), $h = -1.50155$ (right, first row), $h = -1.5$ (left, second row), $h = -1$ (right, second row). The green part shows us the region with possible motion, while the red one is the forbidden region of movement. The two crosses show the location of equilibria.

In Figure 3.1 a first approach to Hill's regions for $K = 0.0015749$ and different values of the energy are shown. For other values of the parameter K the curves have a similar topology. In the particular case of $K = 0.0015749$, $h_1 = -1.50157449$ and $h_2 = -1.49842469$. Notice that for values of the energy below h_1 the region of motion has two components, whereas for bigger values of the energy, the region of motion has only one component, and the inner (around the origin) and outer regions are connected via a bottleneck region around the equilibrium point $\mathcal{L}_1$. Although there exists only one component of motion for $h_1 < h < h_2$, for values of the energy close to h_1 we still refer to the inner and outer regions connected via the bottleneck around $\mathcal{L}_1$. Recall that when $h \geq h_2$ the movement is possible everywhere.

Thanks to this intuitive procedure, we obtain an idea of how the commented regions are. However, Figure 3.1 shows only an approximation of real Hill's regions. For each case, we want to determine the curves delimiting the border of Hill's regions, which are called *zero velocity curves* (zvc).

3.2 Zero Velocity Curves

In order to determine the zvc, we have to find the curves such that, considering h fixed,

$$G(x,y) = h + \frac{y^2}{2} + \frac{x^2}{2} + \frac{1}{r} - Kx = 0. \tag{3.5}$$

This task will be done by implementing the so called *Pseudo-Arc Method*.

3.2.1 Pseudo-Arc Method

The goal of this method is to compute a family of solutions, $X(s)$, of a system. This family of solutions will be called a *branch*. Suppose that we have a solution $X(s_0) = (x_0, y_0)$, where $x_0 \in \mathbb{R}$ and $y_0 \in \mathbb{R}^n$, of the system of n equations

$$G(x,y) = 0.$$

Moreover, suppose that the unitary vector (x_0', y_0') tangent to the family is known and that the Jacobian matrix of G in (x_0, y_0) has rank n (maximal). The method consists in solving the following system,

$$\begin{cases} G(x_1, y_1) & = 0 \\ (x_1 - x_0)x_0' + (y_1 - y_0)y_0' - \Delta s & = 0 \end{cases} \tag{3.6}$$

in order to determine (x_1, y_1), where Δs is given. The introduced system of $n+1$ equations will be written in a short way as

$$F(X) = 0, \tag{3.7}$$

where $X = (x, y) \in \mathbb{R}^{n+1}$.

3.2.1 Remark

- The second equation of system (3.6) says that the projection of vector $(x_1 - x_0, y_1 - y_0)$ over (x_0', y_0') is equal to Δs.
- System (3.6) will be solved using Newton's Method with first approximation taken following the tangent direction to the branch, i.e.

$$(x_1^{(0)}, y_1^{(0)}) = (x_0, y_0) + \Delta s(x_0', y_0').$$

- After obtaining (x_1, y_1), we need (x_1', y_1') in order to predict the next point of the branch. This vector can be found by solving

$$\begin{pmatrix} G_x^1 & G_y^1 \\ x_0' & y_0' \end{pmatrix} \begin{pmatrix} x_1' \\ y_1' \end{pmatrix} = \begin{pmatrix} 0 \\ 1 \end{pmatrix}, \tag{3.8}$$

  where $G_x^1 := G_x(x_1, y_1)$ and $G_y^1 := G_y(x_1, y_1)$. The first equation of (3.8) comes from the derivative of

$$G(X(s)) = G(x(s), y(s)) = 0$$

  with respect to s. The second equation preserves the orientation of the branch. After obtaining (x_1', y_1'), we need to rescale it in order to have an unitary vector.

- This method has advantages over others, because it allows us to calculate the points of the branch even if there are return points.

Using the explained method taking as function G the one defined in (3.5), the new system $F(X) = 0$ has two equations and its solutions are the zero velocity curves of the CP problem for fixed values of K and h.

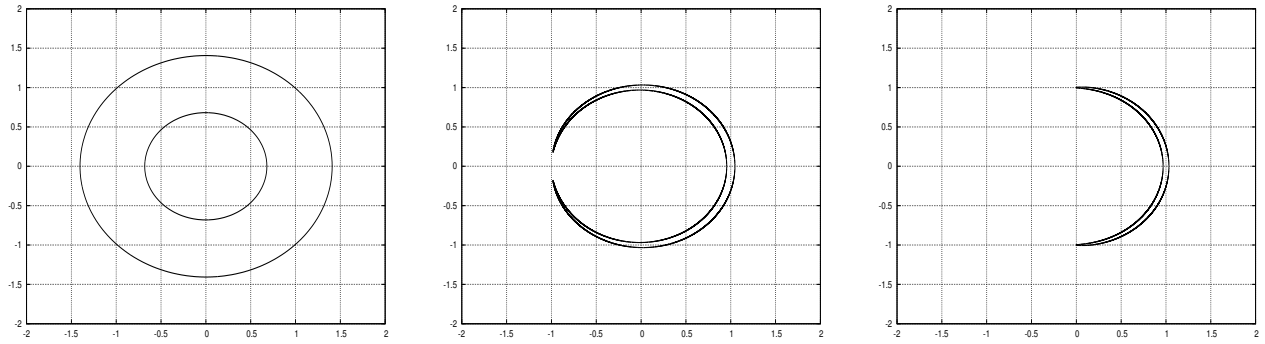

Figure 3.2: Zero velocity curves corresponding to Hill's regions of Figure 3.1. $K = 0.0015749$ and, from left to right: $h = -1.7 < h_1$, $h = -1.50155 \approx h_1$ and $h_1 < h = -1.5 < h_2$.

4 Homoclinic connections to $\mathcal{L}_1$

One could be interested in knowing the local structure of differential equations near equilibrium points. It is not necessary being an expert in Dynamical Systems to have heard something about the local stable and unstable manifolds associated to an equilibrium. Our goal is not giving a complete theory about dynamical concepts, we just want to introduce the fundamental ideas to understand the numerical skeleton that we are trying to construct. For additional information see [2].

4.0.2 Definition Consider the autonomous system (1.19) and let $\mathbf{p}$ be an equilibrium point. Let $\varepsilon > 0$ be given, then the *local stable manifold* associated to $\mathbf{p}$ is

$$W^s(\varepsilon) = \{\mathbf{x} \in \mathbb{R}^n : |\phi(t;\mathbf{x}) - \mathbf{p}| < \varepsilon \text{ for all } t \geq 0\}.$$

Similarly, the *local unstable manifold* associated to $\mathbf{p}$ is

$$W^u(\varepsilon) = \{\mathbf{x} \in \mathbb{R}^n : |\phi(t;\mathbf{x}) - \mathbf{p}| < \varepsilon \text{ for all } t \leq 0\}.$$

4.0.3 Remark Both manifolds are invariant to the flow by definition.

4.0.4 Theorem ***(Local stable manifold for flows)*** *Assume* $\mathbf{f}$ *smooth enough in* $\mathcal{U} \subset \mathbb{R}^n$*, for* $\mathcal{U}$ *an open set. Let* $\mathbf{A} = \mathbf{Df}(\mathbf{p})$ *have* d *eigenvalues with negative real parts and* $n-d$ *eigenvalues with positive real parts. Then for* ε *sufficiently small,* $W^s(\varepsilon)$ *and* $W^u(\varepsilon)$ *are smooth manifolds of dimensions* d *and* $n-d$*, respectively. If* $\mathbf{x} \in W^s(\varepsilon)$ *(respectively,* $\mathbf{x} \in W^u(\varepsilon)$*), then* $\phi(t;\mathbf{x}) \to \mathbf{p}$ *as* $t \to +\infty$ *(respectively,* $\phi(t;\mathbf{x}) \to \mathbf{p}$ *as* $t \to -\infty$*). Actually, there is a smooth, near identity change of coordinates that takes the stable and unstable manifolds to (different) coordinates planes.*

4.0.5 Notation Consider $\sigma_s := \{\lambda \in Spec\ \mathbf{A} | \Re(\lambda) < 0\}$ and $\sigma_u := \{\lambda \in Spec\ \mathbf{A} | \Re(\lambda) > 0\}$, and let $< \sigma_s >$ and $< \sigma_u >$ be the linear subspaces generated by the eigenvectors of the associated eigenvalues in σ_s and σ_u, respectively. One can write $Spec\ \mathbf{A} = \sigma_s \cup \sigma_u$.

4.0.6 Remark $W^s(\varepsilon)$ is tangent to $< \sigma_s >$ at $\mathbf{p}$ and $W^u(\varepsilon)$ is tangent to $< \sigma_u >$ at $\mathbf{p}$. Later we will use this remark in order to find numerically these invariant manifolds.

Theorem (4.0.4) is a local result; so, a natural question to ask is what happens to these manifolds. In fact, they can be continued and their definition can be extended to the following one:

4.0.7 Definition The *(global) stable manifold* is

$$W^s = W^s(\mathbf{p}) = \{\mathbf{x} \in \mathbb{R}^n : \phi(t;\mathbf{x}) \to \mathbf{p} \text{ as } t \to +\infty\},$$

and the *(global) unstable manifold* is

$$W^u = W^u(\mathbf{p}) = \{\mathbf{x} \in \mathbb{R}^n : \phi(t;\mathbf{x}) \to \mathbf{p} \text{ as } t \to -\infty\}.$$

Thanks to these manifolds, we get an idea of the local behaviour around an equilibrium point with hyperbolic part. Later we will see properties of global type.

4.0.8 Example In order to obtain an idea of how these manifolds look, observe again the left hand side of figure 1.1 (a saddle behaviour). That case corresponds to a linear system, for this reason the invariant manifolds are straight lines, being the red one the unstable manifold and the blue one the stable manifold. As we can check, around the equilibrium, the behaviour of the solutions is driven by the one on the manifolds.

4.1 Introduction to the stable and unstable manifolds of the CP problem

Coming back to our system and recalling remark (1.1.17), we realize that we only can study the stable and unstable manifolds of $\mathcal{L}_1$, due to the fact that it is the only unstable equilibrium of the CP system (or the only one with hyperbolic part).

Thanks to lemma (1.1.16) we know that, for all $K > 0$, $\mathcal{L}_1$ is of type center $\times$ saddle, which means that its hyperbolic part has dimension 2 and each invariant manifold has dimension 1, so

$$\begin{aligned} \sigma_s &= \{-a\} \\ \sigma_u &= \{a\}, \end{aligned}$$

being $\pm a$, for $a > 0$, the eigenvalues corresponding to the saddle part. Suppose that v_a and v_{-a} are the eigenvectors associated to the eigenvalues a and $-a$, respectively, so

$$\begin{aligned} < \sigma_s > &= < v_{-a} > \\ < \sigma_u > &= < v_a > . \end{aligned}$$

For simplicity, consider that the eigendirections are unitary,

$$\begin{aligned} v_a &:= \frac{v_a}{||v_a||} \\ v_{-a} &:= \frac{v_{-a}}{||v_{-a}||}. \end{aligned}$$

In order to compute numerically the stable and unstable manifolds we should use remark (4.0.6). First of all, we find an initial condition on the stable manifold and another one on the unstable one, and then, recalling the invariance property (4.0.3), we use Taylor integrator to find the whole manifolds:

$$\text{Initial condition on the stable manifold:} \quad \mathcal{L}_1 + sv_{-a} \tag{4.1}$$

$$\text{Initial condition on the unstable manifold:} \quad \mathcal{L}_1 + sv_a, \tag{4.2}$$

being s small enough ($\approx 10^{-6}$). After knowing the corresponding initial conditions, if we want to obtain the stable manifold we integrate backwards in time, while for the unstable manifold the integration goes forward in time.

In our case, each manifold has two branches, one for each orientation of the eigenvector. Just for simplicity, suppose that the introduced eigenvectors v_a and v_{-a} have a positive y-coordinate.

4.1.1 Notation We will write as W^s_+ the *positive branch* of the stable manifold, or, in other words, the one tangent to v_{-a}. In the same way, we will write as W^u_+ the unstable branch tangent to v_a.

We will write as W^s_- the *negative branch* of the stable manifold, or, in other words, the one tangent to $-v_{-a}$. In the same way, we will write as W^u_- the unstable branch tangent to $-v_a$.

Observe that the names *positive* or *negative branch* depend on the taken sign of the y-coordinate of the eigendirection. See Figure 4.1.

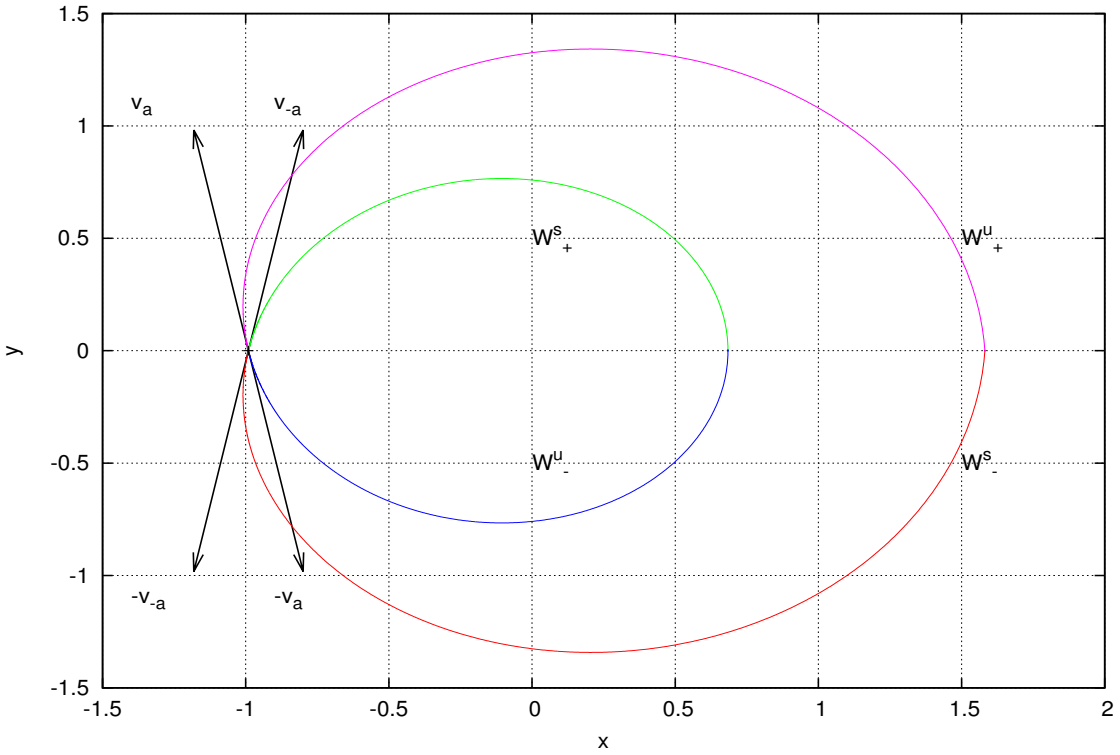

Figure 4.1: (x, y) projection: different branches of the stable and unstable manifolds associated to $\mathcal{L}_1$ when $K = 0.028559865$.

Sometimes we can be in front of a particular situation:

4.1.2 Definition In an autonomous system, it is said that we have a *homoclinic connection* if $W^s(\mathbf{p})$ and $W^u(\mathbf{p})$ intersect.

4.1.3 Remark In an autonomous system, if two orbits intersect, they are the same orbit. Therefore, in our system, we will have a homoclinic connection if a branch of the stable manifold and a branch of the unstable one are the same. Observe that, in Figure 4.1, there are intersections between branches, but as the figure only shows a (x, y)-projection of a 4-dimensional system, they can be different orbits and maybe they are not homoclinic connections.

The following figure shows us an intuitive idea of how a homoclinic connection looks.

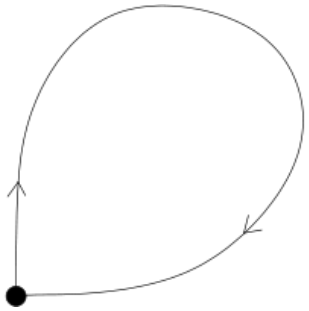

Figure 4.2: Homoclinic connection in a 2-dimensional system.

Along this chapter we consider $\mathcal{L}_1$ and study the existence of homoclinic connections to it, i.e. lemma (1.1.3) gives us an idea of how to compute a type of homoclinic connections: the ones which are symmetric with respect $y = 0$. As a comment, there could be homoclinic connections to $\mathcal{L}_1$ without this symmetry, but now they are not our principal goal. The study that we are going to present has been done in a similar way for the RTBP (see [8]).

4.2 Symmetric homoclinic connections

The existence of symmetric homoclinic orbits is investigated, and thanks to lemma (1.1.3) it is seen that they occur when W^u and W^s intersect at the x-axis perpendicularly (that is, with $x' = 0$). In order to find the values of K such that $\mathcal{L}_1$ has such a connection, we follow the branch W^u_- up to its j intersection with the x-axis and we keep the value of x', that we denote by $x'_j(K)$. Due to the symmetry given in lemma (1.1.3), for each value of K such that the function $x'_j(K) = 0$, the corresponding trajectory has an *orthogonal crossing* to the x-axis and becomes a symmetric homoclinic connection to $\mathcal{L}_1$. Such a connection is in the inner region of the motion around the origin, and we call it an *inner connection*. In order to study *outer connections*, the intersection of the branches W^u_+ and W^s_- should be considered.

During this section, we study in detail the inner connections, and the analogous results for the outer ones are only commented.

4.2.1 Inner connections

First of all, we have implemented, given an initial condition, the first return of the orbit defined by this initial condition to the Poincaré section $y = 0$. The implementation is simple, let Taylor's integrator run until two consecutive steps of the integration with different sign of the y-coordinate are obtained, then an unidimensional Newton's method starts in order to approach the exact instant of time that the orbit needs to reach the Poincaré section. In order to compute the j^{th}-return to the section, we only need to use $j-1$ times more the code of the first return, taking each time the previous return as initial condition.

In our case, given a value of K, our first initial condition is of the form (4.2). Then, at each crossing, x' is computed. For each value of the parameter, we want to study for which values of j there is a homoclinic connection or, equivalently, $x'_j = 0$.

For different values of j, we have computed the function $x'_j(K)$, for $K > 0$. We are not sure about the existence of any value of K such that $x'_1(K) = 0$, because we have studied values of the parameter greater

or equal than 0.001 and $\min_{K\in[0.001,0.16]} |x_1'(K)| \approx 10^{-13}$. While it is difficult to say something about the existence of 1-round symmetric homoclinic connections, there appears a decreasing sequence of values of K with $x_2'(K) = 0$ (look at the following figure).

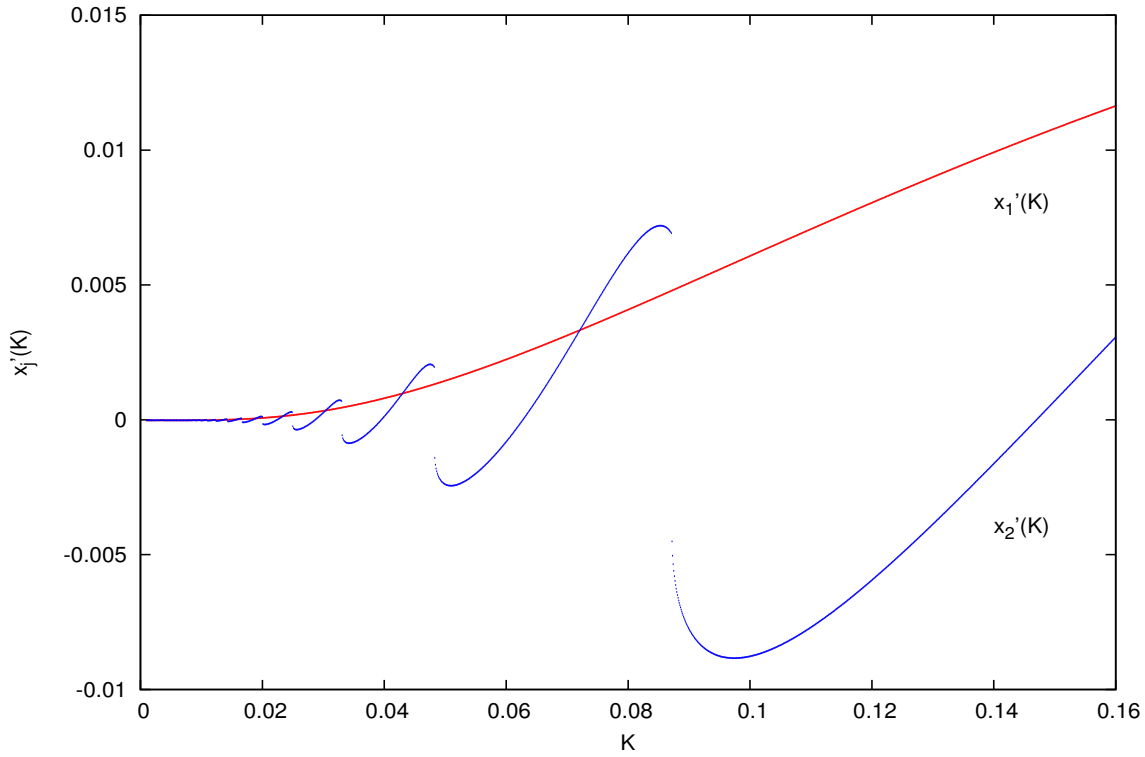

Figure 4.3: Plot of functions $x_j'(K)$, $j = 1, 2$, corresponding, for each K, to the value of the coordinate x' of the point of the orbit of W_-^u of $\mathcal{L}_1$ at its j-th intersection with x-axis.

Each value of K for which $x_2'(K) = 0$ corresponds to a 2-round symmetric homoclinic orbit, and they are called in this way because these connections perform two loops around the origin. Thanks to the previous figure, we can say that there are infinite values of K (tending to zero) for which a 2-round symmetric homoclinic connection to $\mathcal{L}_1$ exists. For example, a homoclinic connection of this kind is performed when $K = 0.02855986$. See Figure 4.4.

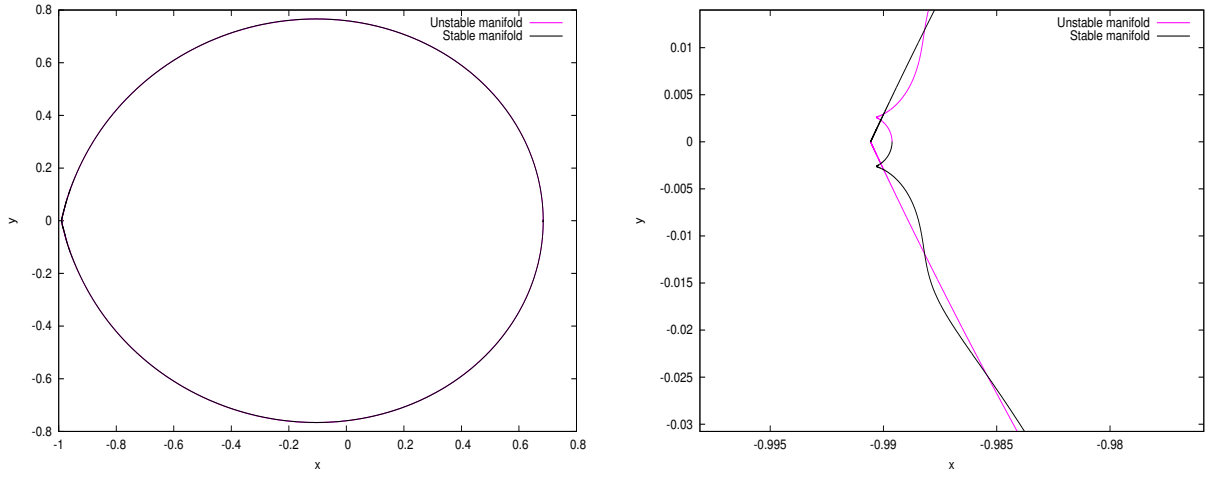

Figure 4.4: Example of a 2-round symmetric homoclinic connection ((x, y) projection) for $K = 0.02855986$. Left: Whole orbit. Right: Zoom of the orbit around $\mathcal{L}_1$.

In addition, as we have commented above, the last connection is located in the inner region of motion, Figure 4.5.

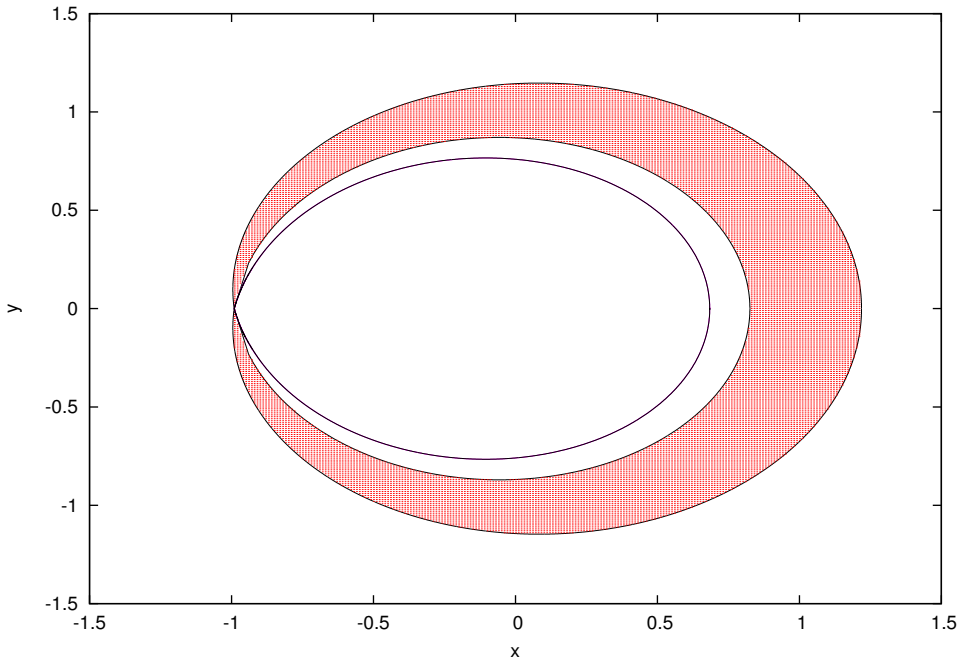

Figure 4.5: Hill's region at $h = h_1$ with a 2-round symmetric homoclinic connection ($K = 0.02855986$) in the inner part.

Figure 4.3 shows that $x_2'(K)$ has infinite discontinuities. In order to justify them, we are going to focus

our attention on $K \in (0.08, 0.096)$ (look at Figure 4.6). In fact, the situation shown in Figure 4.6 is the same as in Figure 4.3, but now the space of the parameter K has been reduced and function $x_3'(K)$ has been added in order to study the third crossing with the x-axis.

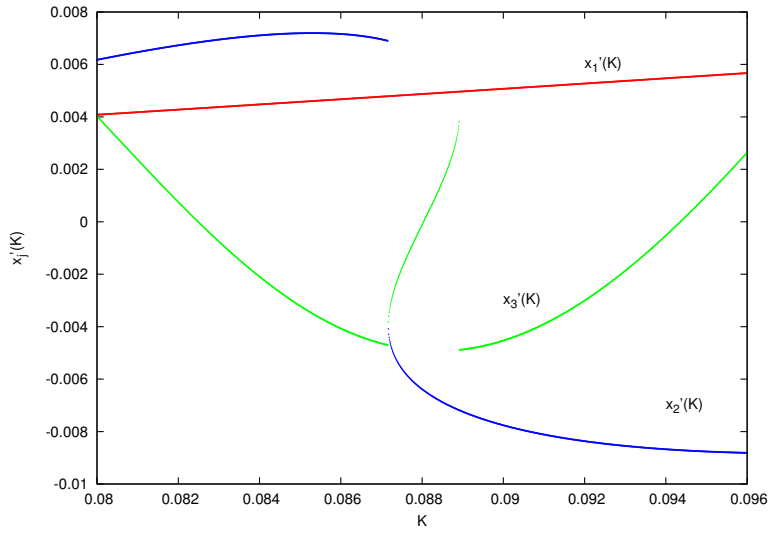

Figure 4.6: In red: $x_1'(K)$. In blue: $x_2'(K)$. In green: $x_3'(K)$.

It is seen that there exists a value $K_h \in (0.08, 0.096)$ such that $x_3'(K_h) = 0$. Computing K_h numerically, we obtain $K_h \approx 0.0880305$.

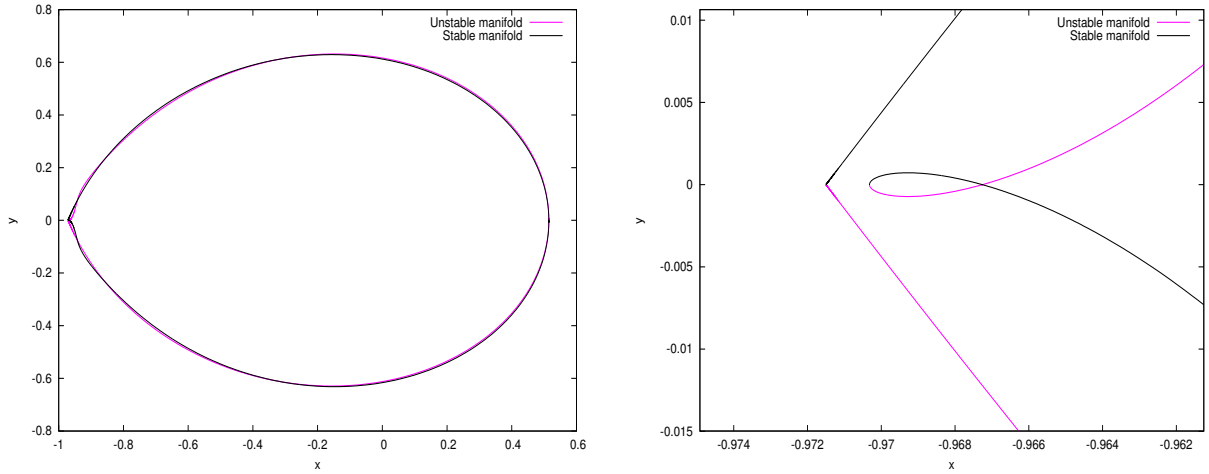

Figure 4.7: 2-round symmetric homoclinic connection ((x, y) projection) for K_h. Left: Whole orbit. Right: Zoom of the orbit around $\mathcal{L}_1$.

On the right hand side of Figure 4.7, we can see that when $K = K_h$ there is a *loop* just after the second return to the x-axis. In fact, in the commented figure, the homoclinic connection takes place in the

third crossing with the Poincaré section, because in the second one $x' < 0$. This loop is the main cause of discontinuities in Figure 4.3. Taking a value of the parameter close to K_h, there are three possible situations: $K < K_h$, $K = K_h$ and $K > K_h$. The situation $K = K_h$ has been performed in Figure 4.7. Let us observe what happens when $K < K_h$ or $K > K_h$.

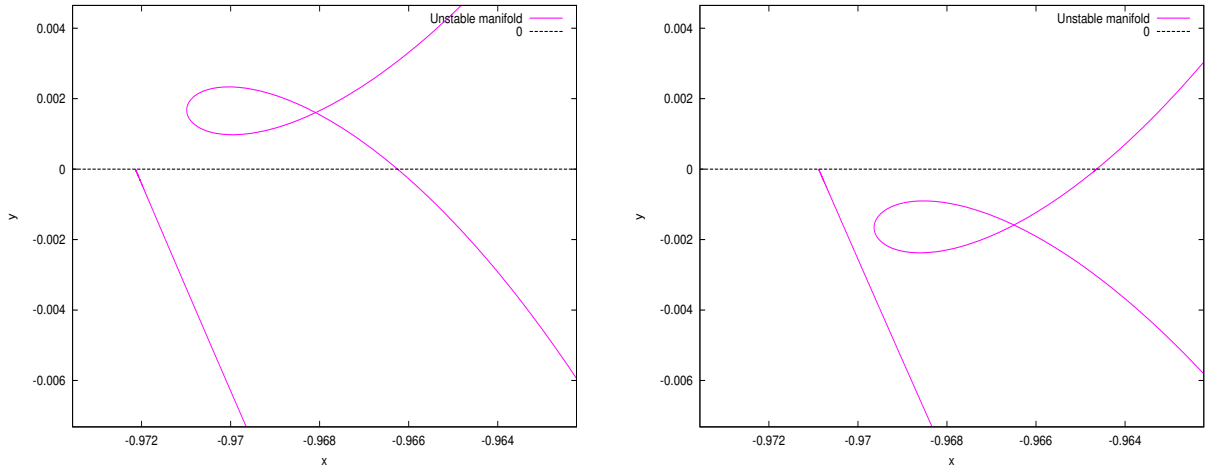

Figure 4.8: Zoom of the unstable manifold around $\mathcal{L}_1$. Second crossing with the x-axis is shown. Left: $K < K_h$. Right: $K > K_h$.

If $K < K_h$, the unstable manifold reaches the x-axis for second time with $x' > 0$, while if $K > K_h$ the second crossing is reached with $x' < 0$. So, the discontinuity of $x_2'(K)$ in (4.6) is the consequence of the movement of the loop. Then, we can say that, each discontinuity of $x_2'(K)$ in Figure 4.3 is a consequence of the existence of a 2-round symmetric homoclinic connection with a loop (like in Figure 4.7).

4.2.2 Outer connections

In the same way that we have shown that there exist an infinity of values of K for which an inner homoclinic connection exists, a similar result follows for the outer connections.

An analogous plot to the one of Figure 4.3 has been computed, observe Figure 4.9. Again, while it is difficult to talk about the existence of 1-round homoclinic connections, there appears a decreasing sequence of values of K with $x_2'(K) = 0$.

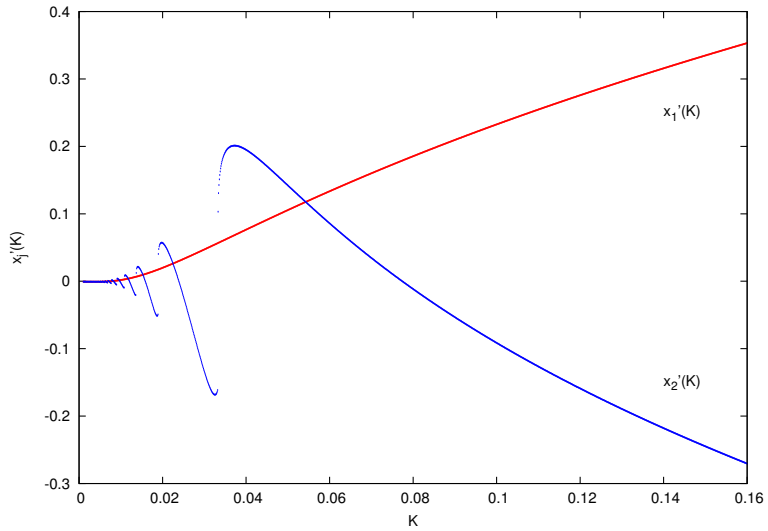

Figure 4.9: Plot of functions $x'_j(K)$, $j = 1, 2$, corresponding, for each K, to the value of the coordinate x' of the point of the orbit of W^u_+ of $\mathcal{L}_1$ at its j-th intersection with x-axis.

5 Variational equations

Consider $\phi_t(\mathbf{x}) = \phi(t, \mathbf{x})$ the solution of system (1.8)-(1.11),

$$\begin{aligned} x' &= p_x + y := f_1(x, y, p_x, p_y) \\ y' &= p_y - x := f_2(x, y, p_x, p_y) \\ p_x' &= p_y - \frac{x}{r^3} - K := f_3(x, y, p_x, p_y) \\ p_y' &= -p_x - \frac{y}{r^3} := f_4(x, y, p_x, p_y), \end{aligned}$$

such that

$$\phi_{t_0}(\mathbf{x}) = \mathbf{x}.$$

The system of *Variational equations of first order* of the previous system can be written, in matrix notation, as

$$\begin{aligned} \begin{pmatrix} \frac{\partial\phi_1}{\partial x} & \frac{\partial\phi_1}{\partial y} & \frac{\partial\phi_1}{\partial p_x} & \frac{\partial\phi_1}{\partial p_y} \\ \frac{\partial\phi_2}{\partial x} & \frac{\partial\phi_2}{\partial y} & \frac{\partial\phi_2}{\partial p_x} & \frac{\partial\phi_2}{\partial p_y} \\ \frac{\partial\phi_3}{\partial x} & \frac{\partial\phi_3}{\partial y} & \frac{\partial\phi_3}{\partial p_x} & \frac{\partial\phi_3}{\partial p_y} \\ \frac{\partial\phi_4}{\partial x} & \frac{\partial\phi_4}{\partial y} & \frac{\partial\phi_4}{\partial p_x} & \frac{\partial\phi_4}{\partial p_y} \end{pmatrix}' &= \begin{pmatrix} D_x f_1 & D_y f_1 & D_{p_x} f_1 & D_{p_y} f_1 \\ D_x f_2 & D_y f_2 & D_{p_x} f_2 & D_{p_y} f_2 \\ D_x f_3 & D_y f_3 & D_{p_x} f_3 & D_{p_y} f_3 \\ D_x f_4 & D_y f_4 & D_{p_x} f_4 & D_{p_y} f_4 \end{pmatrix} \begin{pmatrix} \frac{\partial\phi_1}{\partial x} & \frac{\partial\phi_1}{\partial y} & \frac{\partial\phi_1}{\partial p_x} & \frac{\partial\phi_1}{\partial p_y} \\ \frac{\partial\phi_2}{\partial x} & \frac{\partial\phi_2}{\partial y} & \frac{\partial\phi_2}{\partial p_x} & \frac{\partial\phi_2}{\partial p_y} \\ \frac{\partial\phi_3}{\partial x} & \frac{\partial\phi_3}{\partial y} & \frac{\partial\phi_3}{\partial p_x} & \frac{\partial\phi_3}{\partial p_y} \\ \frac{\partial\phi_4}{\partial x} & \frac{\partial\phi_4}{\partial y} & \frac{\partial\phi_4}{\partial p_x} & \frac{\partial\phi_4}{\partial p_y} \end{pmatrix} \\ &= \begin{pmatrix} 0 & 1 & 1 & 0 \\ -1 & 0 & 0 & 1 \\ \frac{2x^2-y^2}{r^5} & \frac{3xy}{r^5} & 0 & 1 \\ \frac{3xy}{r^5} & \frac{2y^2-x^2}{r^5} & -1 & 0 \end{pmatrix} \begin{pmatrix} \frac{\partial\phi_1}{\partial x} & \frac{\partial\phi_1}{\partial y} & \frac{\partial\phi_1}{\partial p_x} & \frac{\partial\phi_1}{\partial p_y} \\ \frac{\partial\phi_2}{\partial x} & \frac{\partial\phi_2}{\partial y} & \frac{\partial\phi_2}{\partial p_x} & \frac{\partial\phi_2}{\partial p_y} \\ \frac{\partial\phi_3}{\partial x} & \frac{\partial\phi_3}{\partial y} & \frac{\partial\phi_3}{\partial p_x} & \frac{\partial\phi_3}{\partial p_y} \\ \frac{\partial\phi_4}{\partial x} & \frac{\partial\phi_4}{\partial y} & \frac{\partial\phi_4}{\partial p_x} & \frac{\partial\phi_4}{\partial p_y} \end{pmatrix} \end{aligned} \tag{5.1}$$

with initial condition

$$\left.\frac{\partial\phi_t(\mathbf{x})}{\partial\mathbf{x}}\right|_{t=t_0} = \mathbf{Id}. \tag{5.2}$$

In order to compute the Variational solutions, it is needed to consider the system of 20 ODE formed by adding the Variational equations to the CP system. Applying Taylor's integrator to the *extended* problem, we will obtain the solutions of the Variational system numerically.

6 Dynamics from a global point of view

In this chapter we describe, by means of Poincaré section plots (PSP), the dynamics of system (1.8)-(1.11) from a *global* point of view, analyzing the different invariant objects that take place. We begin recalling the dynamics of the two-body problem (when $K = 0$), which is the simplest case, giving first an introduction to the problem and some of its properties: equilibrium points, regions of motion and different types of orbits. After introducing all of these topics one should be able to understand the Poincaré section plots that are going to be shown for $K = 0$. Later we will show the evolution of these plots for $K > 0$.

We consider the Poincaré section $\Sigma = \{\mathbf{x} : x' = 0 \text{ and } y' < 0\}$. A PSP is computed as follows: for a fixed value of the energy h we take a set of initial conditions over Σ, $x = x_0$, $y = 0$, $x' = 0$ and $y' = y_0$, where y_0 has been obtained from (3.2) using the known value of h,

$$y_0 = -\sqrt{2h + x_0^2 + \frac{2}{|x_0|} - 2Kx_0}, \tag{6.1}$$

and varying x_0. For each initial condition, we integrate the corresponding orbit up to n intersections with the section $x' = 0$ (normally, $n = 800$) and we plot the (x, y) projection of the n intersection points which are in Σ (or, in other words, $y' < 0$).

6.1 The two-body problem: $K = 0$

In remark (1.1.2) we have commented that when $K = 0$ we are in front of the two-body problem, but so far we have not said anything about this problem. In this section we want to introduce the commented problem and some interesting facts about it.

6.1.1 Description of the problem

Consider two masses m_1 and m_2 in the space and their positions $\mathbf{r_1}$ and $\mathbf{r_2}$ which connect them to the origin $\mathcal{O}$ of an inertial system of reference. The description of the motion of the system of the two mass particles moving according to their mutual gravitational attraction is known as the *two-body problem*.

According to Newton's law of universal gravitation, the force of attraction between the particles is $Gm_1m_2r^{-2}$, where G is the constant of gravitation and $r = |\mathbf{r_2} - \mathbf{r_1}|$. Now, applying Newton's second law, we obtain the following system of differential equations:

$$\begin{cases} m_1\ddot{\mathbf{r_1}} = \frac{Gm_1m_2}{r^2}\frac{\mathbf{r_2}-\mathbf{r_1}}{r}, \\ m_2\ddot{\mathbf{r_2}} = \frac{Gm_2m_1}{r^2}\frac{\mathbf{r_1}-\mathbf{r_2}}{r}, \end{cases}$$

or

$$\begin{cases} \ddot{\mathbf{r_1}} = \frac{Gm_2}{r^3}(\mathbf{r_2} - \mathbf{r_1}), \\ \ddot{\mathbf{r_2}} = -\frac{Gm_1}{r^3}(\mathbf{r_2} - \mathbf{r_1}), \end{cases} \tag{6.2}$$

and it is assumed that initial values of $\mathbf{r_1}$, $\mathbf{r_2}$, $\dot{\mathbf{r_1}}$, $\dot{\mathbf{r_2}}$ are given. There are six second order differential equations. Substracting the first equation of (6.2) from the second and denoting $\mathbf{r_2} - \mathbf{r_1}$ by $\mathbf{r}$, we find that

$$\ddot{\mathbf{r}} = -\frac{G(m_1 + m_2)}{r^3}\mathbf{r} := -\frac{\mu}{r^3}\mathbf{r} \tag{6.3}$$

which describes the motion of one body with respect to the other body.

6.1.1 Remark (The central force problem)

The description of the motion of a particle of mass m which is attracted to a fixed center $\mathcal{O}'$ by a force $mf(r)$ which is proporcional to the mass and depends only on the distance r between the particle and $\mathcal{O}'$ is called *the central force problem.*

Indicating the position of the mass by the vector $\mathbf{r}$ directed from $\mathcal{O}'$ and using Newton's second law, the formulation of the problem is as follows

$$m\ddot{\mathbf{r}} = -\frac{mf(r)}{r}\mathbf{r} \Leftrightarrow \ddot{\mathbf{r}} = -\frac{f(r)}{r}\mathbf{r} \tag{6.4}$$

Comparing system (6.4) with system (6.3), one can see that we have reduced our problem to the central force problem with $f(r) = \mu r^{-2}$. Thanks to this relation, we can say that each particle moves as if it were a unit mass attracted to a fixed center located at the other mass.

Thanks to the idea of realtive motion and (6.3), we take a suitable units of time, length and mass, and consider $m_1 = 1$, $m_2 \approx 0$ and $G = 1$. So, from now $\mu = 1$ and system (6.3) becomes

$$\ddot{\mathbf{r}} = -\frac{\mathbf{r}}{r^3}. \tag{6.5}$$

We are going to focus our attention to the planar case of the two-body problem (remember that we are also studying the planar CP problem), so $Z = 0$ and we can rewrite (6.5) in coordinates as

$$\begin{cases} \ddot{X} = -\frac{X}{(X^2+Y^2)^{\frac{3}{2}}}, \\ \ddot{Y} = -\frac{Y}{(X^2+Y^2)^{\frac{3}{2}}} \end{cases} \tag{6.6}$$

6.1.2 Remark (X, Y) coordinates refer to a system of coordinates with fixed axes (sidereal coordinates), with $(0, 0)$ the position of m_1 (relative motion). Therefore (X, Y) represents the relative motion of m_2 with respect m_1.

Synodic system of coordinates

The main idea of this section is to change system (6.6) to a rotating (synodic) system of coordinates (x, y),

$$\begin{pmatrix} X \\ Y \end{pmatrix} = \begin{pmatrix} \cos t & -\sin t \\ \sin t & \cos t \end{pmatrix} \begin{pmatrix} x \\ y \end{pmatrix}. \tag{6.7}$$

Consider

$$\begin{aligned} Z &= X + iY, \\ z &= x + iy, \end{aligned}$$

then $Z = ze^{it}$. As

$$\dot{Z} = \dot{z}e^{it} + ize^{it} = (\dot{z} + iz)e^{it},$$

we have that

$$\ddot{Z} = (\ddot{z} + i\dot{z})e^{it} + (\dot{z} + iz)ie^{it} = \underbrace{(\ddot{z} + 2i\dot{z} - z)e^{it}}_{\text{acceleration in synodic coord.}}. \tag{6.8}$$

As $X + iY = (x + iy)(\cos t + i \sin t) = (x + iy)e^{it}$, we also have that

$$\begin{aligned} \ddot{Z} = \ddot{X} + i\ddot{Y} &= -\left(\frac{X}{(X^2+Y^2)^{\frac{3}{2}}} + i\frac{Y}{(X^2+Y^2)^{\frac{3}{2}}}\right) \\ &= -\frac{1}{(X^2+Y^2)^{\frac{3}{2}}}(X + iY) \\ &= -\frac{1}{(x^2+y^2)^{\frac{3}{2}}}(x + iy)e^{it}, \end{aligned} \tag{6.9}$$

so, equating (6.8) and (6.9),

$$\ddot{z} + 2i\dot{z} - z = -\frac{1}{(x^2+y^2)^{\frac{3}{2}}}(x + iy),$$

and the following is deduced:

$$\left.\begin{aligned} \ddot{x} - 2\dot{y} - x &= -\tfrac{x}{(x^2+y^2)^{\frac{3}{2}}} \\ \ddot{y} + 2\dot{x} - y &= -\tfrac{y}{(x^2+y^2)^{\frac{3}{2}}} \end{aligned}\right\} \overset{r=\sqrt{x^2+y^2}}{\Leftrightarrow} \left\{\begin{aligned} \ddot{x} - 2\dot{y} &= x - \tfrac{x}{r^3} \\ \ddot{y} + 2\dot{x} &= y - \tfrac{y}{r^3} \end{aligned}\right\} \tag{6.10}$$

Therefore the equations of motion of the two-body problem in synodic coordinates are

$$\left.\begin{aligned} \ddot{x} - 2\dot{y} &= x - \tfrac{x}{r^3} = \tfrac{\partial \Omega}{\partial x} \\ \ddot{y} + 2\dot{x} &= y - \tfrac{y}{r^3} = \tfrac{\partial \Omega}{\partial y} \end{aligned}\right\}, \tag{6.11}$$

being $\Omega(x, y) = \frac{1}{2}(x^2 + y^2) + \frac{1}{r}$.

Introducing the following variables (x_1, x_2: positions, y_1, y_2: momenta),

$$\begin{cases} x_1 = x \\ x_2 = y \\ y_1 = \dot{x} - y \\ y_2 = \dot{y} + x \end{cases} \tag{6.12}$$

and using (6.11), we obtain the following 1^{st} order system of ODE for the two-body problem,

$$\begin{aligned} \dot{x_1} &= y_1 + x_2, && (6.13)\\ \dot{x_2} &= y_2 - x_1, && (6.14)\\ \dot{y_1} &= y_2 - x_1 + \frac{\partial \Omega}{\partial x_1} = y_2 - \frac{x_1}{r^3}, && (6.15)\\ \dot{y_2} &= -y_1 - x_2 + \frac{\partial \Omega}{\partial x_2} = -y_1 - \frac{x_2}{r^3}, && (6.16) \end{aligned}$$

with Hamiltonian

$$\mathcal{H}' = \mathcal{H}'(x_1, x_2, y_1, y_2) = \frac{1}{2}(y_1^2 + y_2^2) - x_1 y_2 + x_2 y_1 - \frac{1}{r}. \quad (6.17)$$

6.1.3 Remark System (6.13)-(6.16) coincides with system (1.8)-(1.11) when $K = 0$.

Observe that the two-body problem has two first integrals:

6.1.4 Proposition *$\mathcal{H}'$ is a first integral of system (6.13)-(6.16).*

Proof: Observe that

$$\begin{aligned} \frac{d\mathcal{H}'}{dt}(\mathbf{x}(t), \mathbf{y}(t)) &= \sum_{k=1}^{2} \left(\mathcal{H}'_{x_k} \dot{x_k}(t) + \mathcal{H}'_{y_k} \dot{y_k}(t) \right) \\ &= \sum_{k=1}^{2} \left(\mathcal{H}'_{x_k} \mathcal{H}'_{y_k} - \mathcal{H}'_{y_k} \mathcal{H}'_{x_k} \right) \\ &= 0. \end{aligned}$$

□

6.1.5 Proposition *The angular momentum is a first integral of system (6.13)-(6.16).*

Proof: The angular momentum in sidereal coordinates is given by

$$M = \begin{pmatrix} X \\ Y \end{pmatrix} \wedge \begin{pmatrix} \dot{X} \\ \dot{Y} \end{pmatrix} = X\dot{Y} - \dot{X}Y.$$

Let us change the expression of M into synodic coordinates. Remember the rotation

$$\begin{cases} X = x\cos t - y \sin t, \\ Y = x \sin t + y \cos t, \end{cases}$$

and thanks to it,

$$\begin{aligned} \dot{X} &= \dot{x}\cos t - x \sin t - \dot{y} \sin t - y \cos t \\ \dot{Y} &= \dot{x} \sin t + x \cos t + \dot{y} \cos t - y \sin t. \end{aligned}$$

Then, M becomes

$$\begin{aligned} M = X\dot{Y} - \dot{X}Y &= (x\cos t - y \sin t)(\dot{x} \sin t + x \cos t + \dot{y} \cos t - y \sin t) - \\ &- (\dot{x}\cos t - x \sin t - \dot{y} \sin t - y \cos t)(x \sin t + y \cos t) \\ &= x^2 + y^2 - x\dot{y} - y\dot{x}. \end{aligned}$$

Introducing the variables (6.12),

$$\begin{aligned} x &= x_1, \\ y &= x_2, \\ \dot{x} &= y_1 + x_2, \\ \dot{y} &= y_2 - x_1, \end{aligned}$$

and we obtain

$$M = x_1^2 + x_2^2 + x_1 y_2 - x_1^2 - x_2 y_1 - x_2^2 = x_1 y_2 - x_2 y_1,$$

which is the expression of M in *position-momentum* variables.

In order to see that M is a first integral of system (6.13)-(6.16) we have to show that $\frac{dM}{dt}(\mathbf{x}(t), \mathbf{y}(t)) = 0$.

$$\begin{aligned} \frac{dM}{dt}(\mathbf{x}(t), \mathbf{y}(t)) &= M_{x_1}\mathcal{H}'_{y_1} - M_{y_1}\mathcal{H}'_{x_1} + M_{x_2}\mathcal{H}'_{y_2} - M_{y_2}\mathcal{H}'_{x_2} \\ &= y_2(y_1 + x_2) + x_2\left(-y_2 + \frac{x_1}{(x_1^2 + x_2^2)^{3/2}}\right) - y_1(y_2 - x_1) - x_1\left(y_1 + \frac{x_2}{(x_1^2 + x_2^2)^{3/2}}\right) \\ &= 0. \end{aligned}$$

□

6.1.2 Equilibria of the two-body problem

In section 1.1.2 we have been studying the equilibrium points of the CP problem. As it is already known, when $K = 0$ we are in front of the two-body problem, so we can use equations (1.16)-(1.17) after replacing the parameter K by 0 in order to find the equilibria of the two-body problem. Therefore the system that must be studied is the following one:

$$\begin{cases} y - \frac{y}{r^3} = y\left(1 - \frac{1}{r^3}\right) = 0 \Leftrightarrow \ y = 0 \text{ or } r = 1 \\ x - \frac{x}{r^3} = x\left(1 - \frac{1}{r^3}\right) = 0 \Leftrightarrow \ x = 0 \text{ or } r = 1 \end{cases}$$

As in the point $(0, 0, 0, 0)$ the system has a singularity, the only equilibria of the two-body problem are the points on the unitary circle. Figure 6.1 shows the unitary circle of equilibrium points and the two equilibrium points $\mathcal{L}_1$ and $\mathcal{L}_2$ of the CP problem when $K \neq 0$. As we can see, when K goes to 0 the two points tend to approach the unitary circle.

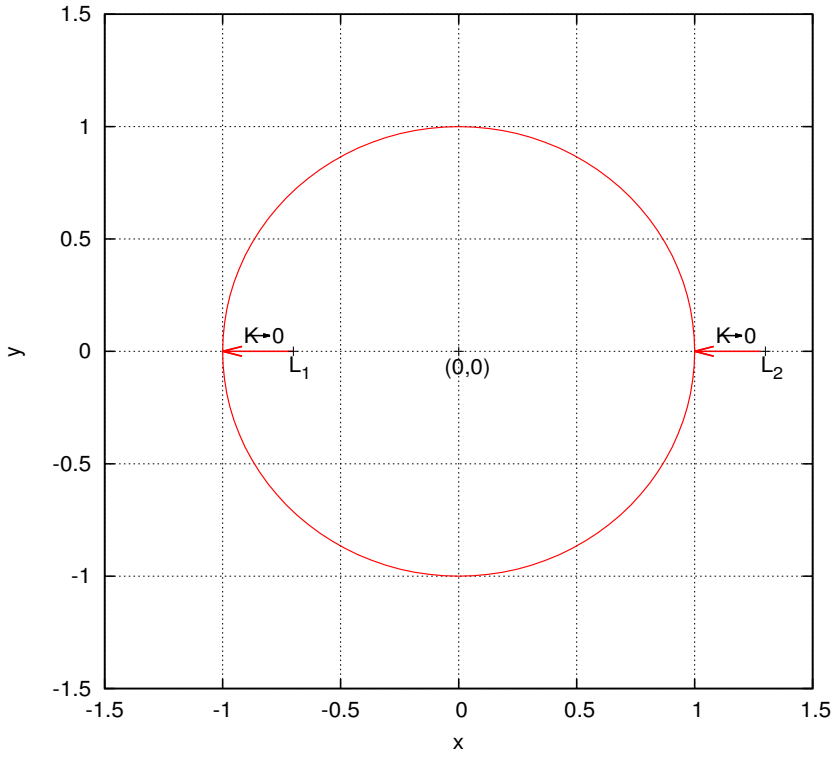

Figure 6.1: In red we can see the equilibria of the CP problem when $K = 0$. The figure shows the evolution, as K approaches 0, of the two equilibrium points of the CP when $K \neq 0$.

6.1.3 Hill's Regions when $K = 0$

In chapter 3 we have been studying the Hill's regions of the CP problem when $K \neq 0$, having only two equilibrium points. In this section we want to present an analitical reasoning about the topologically different Hill's regions that one can have in the two-body problem, in other words, when $K = 0$. In order to do this we can use known results from chapter 3. Thanks to expression (3.4), the points where the movement is possible in the two-body problem have to satisfy the following inequality

$$h + \frac{y^2}{2} + \frac{x^2}{2} + \frac{1}{r} = \underbrace{h}_{h:=\frac{-C}{2}} + \Omega(x,y) \geq 0 \Leftrightarrow 2\Omega(x,y) - C \geq 0 \tag{6.18}$$

being h a fixed value of the energy level. So, the zero velocity curves when $K = 0$ are given by

$$C = 2\Omega(x,y), \tag{6.19}$$

being C a known constant.

6.1.6 Remark C is called the *Jacobi constant*.

In an equilibrium point $(x, y, \dot{x}, \dot{y}) = (\cos\theta, \sin\theta, 0, 0)$, $\theta \in [0, 2\pi)$,

$$C = (1 + 2) + 0 = 3,$$

so we are going to distinguish three different cases: $C > 3$, $C = 3$ and $C < 3$. Observe that the expression (6.19) for the zvc when $K = 0$ can be rewritten as

$$r^2 + \frac{2}{r} - C = 0 \Leftrightarrow r^3 - Cr + 2 = 0, \tag{6.20}$$

and the possible regions of motion satisfy

$$r^3 - Cr + 2 \geq 0. \tag{6.21}$$

Let us study the function $f(r) = r^3 - Cr + 2$ when $r > 0$. Observe that

$$\begin{cases} f(0) = 2, & \\ f'(r) = 3r^2 - C = 0 & \Leftrightarrow r = (+)\sqrt{\frac{C}{3}}, \\ f''(r) = 6r & \Rightarrow r = \sqrt{\frac{C}{3}} \text{ is a local minimum with } f\left(\sqrt{\frac{C}{3}}\right) = -\frac{2C}{3}\sqrt{\frac{C}{3}} + 2\Big|_{C=3} = 0. \end{cases} \tag{6.22}$$

Thanks to (6.22) we deduce that, depending on the value of C, the function f looks as in the following figure.

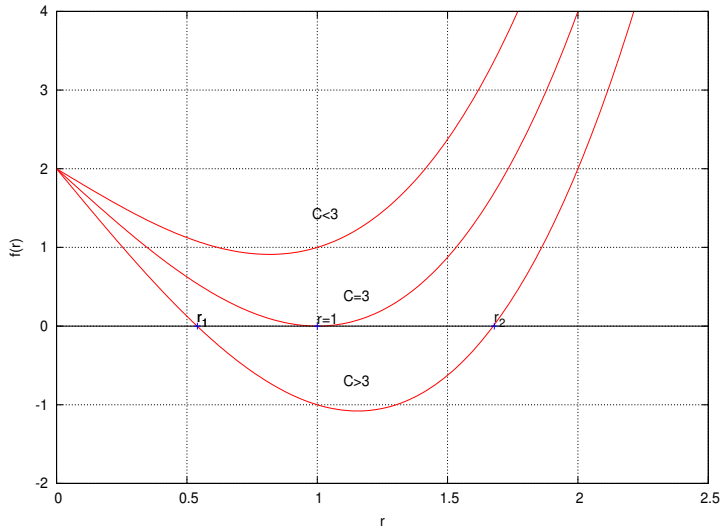

Figure 6.2: Different cases that we can have depending on the value of C.

As the Hill's region for the two-body problem is given by

$$\begin{aligned} \mathcal{R}_H &= \{(x, y) \in \mathbb{R}^2 \text{ such that } 2\Omega(x, y) - C \geq 0\} \\ &= \{(x, y) \in \mathbb{R}^2 \text{ such that } f(r) \geq 0\}, \end{aligned}$$

we can do the following observations thanks to Figure 6.2:

- If $C > 3$, we know that all the points with $r(x, y) \in [0, r_1] \cup [r_2, +\infty)$ can be reached, so the motion is forbidden in a ring.
- If $C = 3$, the zvc is $r(x, y) = 1$, and $\mathcal{R}_H = \mathbb{R}^2$.

- If $C < 3$, there is not zvc and the Hill's region is all the plane (x, y).

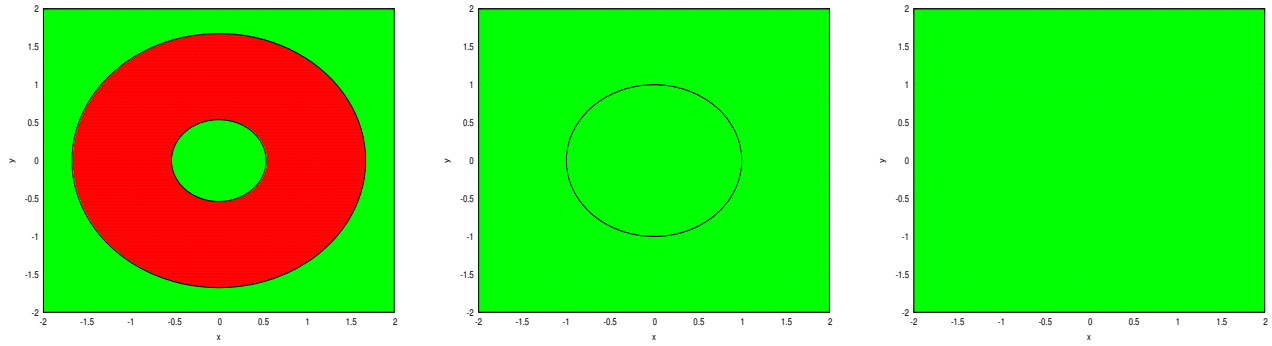

Figure 6.3: Hill's regions in (x, y) coordinates of the two-body problem (CP problem when $K = 0$):$C > 3$, $C = 3$ and $C < 3$, respectively. The green part shows us the region with possible motion, while the red one is the forbidden region of movement. The zero velocity curves are shown in black.

6.1.4 Rotating ellipses, parabolas and hyperbolas

The orbits of the two-body problem in sidereal coordinates (X, Y) are ellipses, parabolas or hyperbolas, while the RTBP presents a higher degree of complexity. For this reason, when we introduce a rotating system in the two-body problem, the dynamics is given by rotating ellipses, parabolas and hyperbolas.

In order to compute these different types of orbits, we take the following initial conditions:

Rotating ellipses

For the case of an ellipse in sidereal coordinates:

$$\begin{cases} X = a(1-e)\cos\alpha \\ Y = a(1-e)\sin\alpha \\ \dot{X} = \mp\sqrt{\frac{1+e}{a(1-e)}}\sin\alpha \\ \dot{Y} = \pm\sqrt{\frac{1+e}{a(1-e)}}\cos\alpha \end{cases} \tag{6.23}$$

where $a > 0$ is the semi-major axis, $e < 1$ is the eccentricity and $\alpha \in [0, 2\pi)$. Observe that $r_{peri} = a(1-e)$ and $v_{peri} = \sqrt{\frac{1+e}{a(1-e)}}$ are the modulus of the position and the velocity of the perihelion, respectively. In order to obtain the initial condition of a rotating ellipse, we have to apply the following change of variables to the sidereal initial condition:

$$\begin{cases} x_1 = x = X \\ x_2 = y = Y \\ y_1 = \dot{x} - y = \dot{X} \\ y_2 = \dot{y} + x = \dot{Y} \end{cases} \tag{6.24}$$

6.1.7 Remark If we are interested in computing orbits at a certain level of energy C, taking as input a and C, it is not difficult to show that the eccentricity e is given by

$$e = \sqrt{1 - \frac{1}{4a}\left[\frac{1}{a} - C\right]^2}. \tag{6.25}$$

(Use the definition of the Hamiltonian of the two-body problem, see expression (6.17), and remember that $C = -2h$)

In order to determine the sign of the velocity at the perihelion we use the sidereal energy. As in this case $e < 1$, the sidereal energy is given by

$$-\frac{1}{2a} = \mathcal{H}' + M = -\frac{C}{2} + M,$$

which means that

$$-\frac{1}{2a} + \frac{C}{2} = M.$$

Assuming a and C known, we obtain the value of M and, consequently, the sign of the velocity.

For more information about the terminology of elliptic orbits see [10].

Rotating parabolas

For the case of a parabola in sidereal coordinates:

$$\begin{cases} X = r_{peri}\cos\alpha \\ Y = r_{peri}\sin\alpha \\ \dot{X} = \mp\sqrt{\frac{2}{r_{peri}}}\sin\alpha \\ \dot{Y} = \pm\sqrt{\frac{2}{r_{peri}}}\cos\alpha \end{cases} \tag{6.26}$$

Again, in order to obtain the initial condition of a rotating parabola (initial condition in the synodic system of coordinates) we apply the change of variables (6.24) to the intial condition (6.26).

6.1.8 Remark If we want to restrict the parabola (6.26) to a certain level of energy C, we must take $r_{peri} = \frac{C^2}{8}$.

In the parabolic case the sidereal energy at the perihelion is 0, so

$$\frac{C}{2} = M,$$

and the sign of the velocity at the perihelion is determined.

Rotating hyperbolas

For the case of a hyperbola in sidereal coordinates:

$$\begin{cases} X = a(e-1)\cos\alpha \\ Y = a(e-1)\sin\alpha \\ \dot{X} = \mp\sqrt{\frac{2}{a(e-1)} + \frac{1}{a}}\sin\alpha \\ \dot{Y} = \pm\sqrt{\frac{2}{a(e-1)} + \frac{1}{a}}\cos\alpha \end{cases} \tag{6.27}$$

Again, in order to obtain the initial condition of a rotating hyperbola we apply the change of variables (6.24) to the initial condition (6.27).

6.1.9 Remark If we are interested in computing orbits at a certain level of energy C, taking as input a and C, it is not difficult to show that the eccentricity e is given by

$$e = \sqrt{1 + \frac{1}{4a}\left[\frac{1}{a} + C\right]^2}. \tag{6.28}$$

As in this case $e > 1$, the sidereal energy at the perihelion is given by

$$\frac{1}{2a} = \mathcal{H}' + M = -\frac{C}{2} + M,$$

which means that

$$\frac{1}{2a} + \frac{C}{2} = M.$$

Assuming a and C known, we obtain the value of M and, consequently, the sign of the velocity.

This method to compute rotating ellipses, parabolas and hyperbolas will be applied in the next section to find numerically this type of orbits when the parameter of our problem is zero.

6.1.5 Poincaré section plots when $K = 0$

After all of this theory about the two-body problem, we are ready to deal with the Poincaré section plots and their meaning.

Let us begin by studying the PSP when $K = 0$. In the last section we have seen that if $h < -\frac{3}{2} = -1.5$ ($C > 3$) the (x, y)-region of motion has two components; if $K = 0$ this fact is shown, for example, when $h = -1.7$ (see left hand side of Figure 6.3).

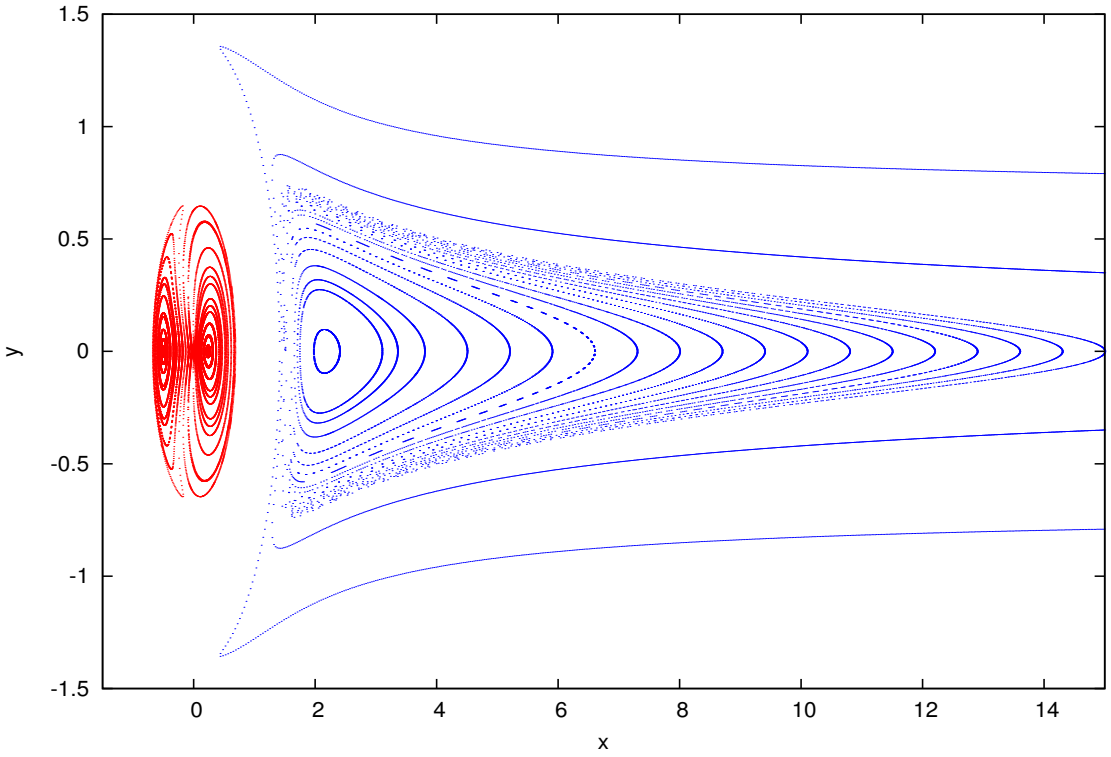

Figure 6.4: PSP when $K = 0$ and $h = -1.7 < h_1$. Points (x, y) on Σ. The movement in the inner component of motion has been plotted in red, while in the unbounded component of motion the behaviour appears in blue.

As we have seen at the beginning of section 6.1, when $K = 0$ we are in front of the rotating two-body problem, which is an integrable problem and the possible orbits come simply from the rotation of ellipses, parabolas or hyperbolas. Thanks to the commented result, let us explain in detail Figure 6.4. The bounded orbits of Figure 6.4 correspond to rotating ellipses which are either periodic or quasiperiodic orbits, seen as fixed points or invariant curves in the PSP (see Figure 6.5), while the rotating parabolas or rotating hyperbolas correspond to the unbounded sets on the PSP. The limit (or boundary) between the bounded and the unbounded orbits in Figure 6.4 corresponds to the parabolic orbit that exists for the value of the energy used in the PSP (in this case, $h = -1.7$).

On one hand, there are invariant curves around the origin corresponding to orbits inside the bounded component of Hill's region, on the other hand, there are invariant curves corresponding to rotating ellipses in the unbounded component of the Hill's region. Such invariant curves are responsible for the *inverted bell* shape of the PSP (in blue in Figure 6.4). Left hand side of Figure 6.5 shows us the main periodic orbit in the outer region of motion of the PSP 6.4.

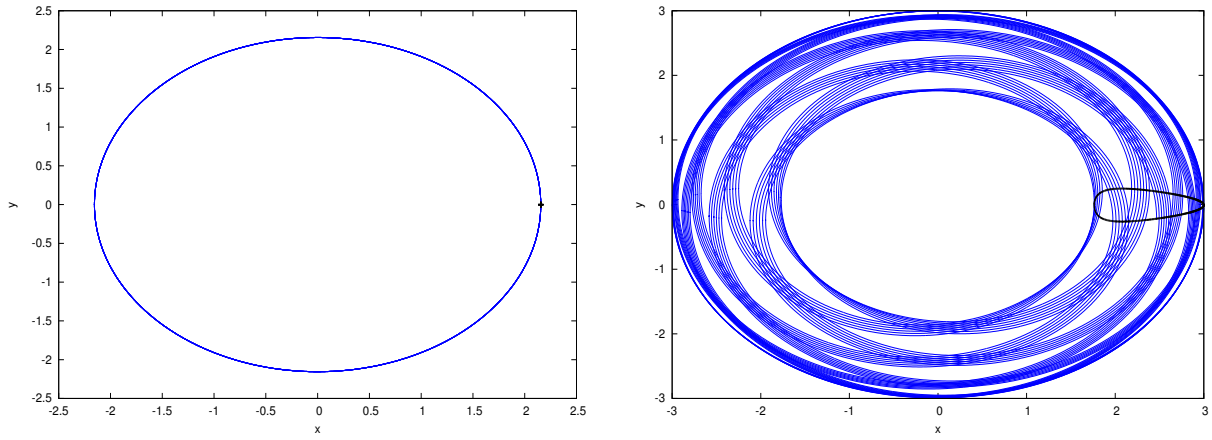

Figure 6.5: Orbits obtained from the rotation of ellipses. In black: (x, y) projection on the PSP. In blue: whole orbit. Left: fixed point in PSP $\leftrightarrow$ periodic orbit. Right: invariant curve in PSP $\leftrightarrow$ quasiperiodic orbit. The two shown behaviours are located in the unbounded region of motion.

We also show how the rotating parabolas and hyperbolas look. See Figure 6.6.

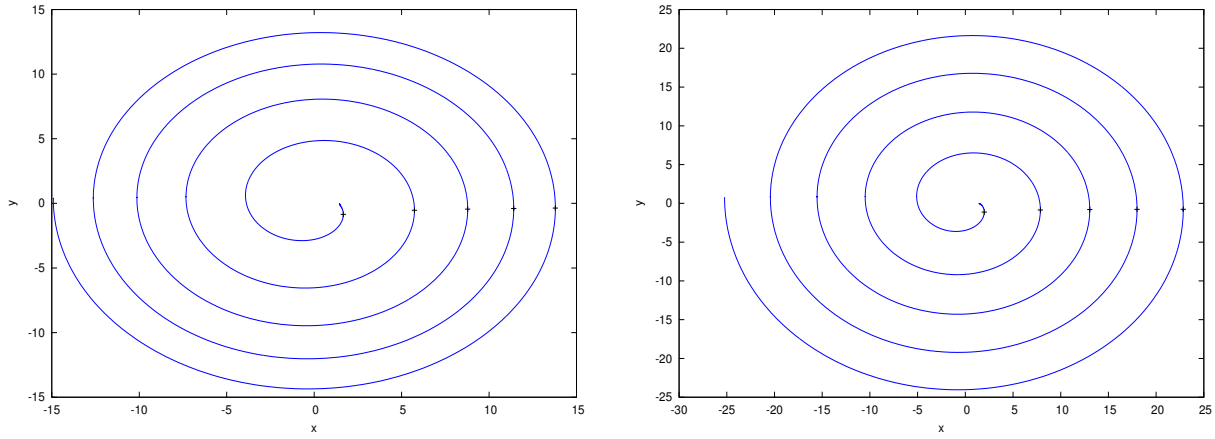

Figure 6.6: Orbits obtained from the rotation of a parabola and the rotation of a hyperbola, respectively. In black: (x, y) projection on the PSP. In blue: whole orbit.

Thanks to this explanation one can say that in the two-body problem the dynamics is simple, in the sense that all the types of orbits that one can have are known. The situation becomes more complicated when $K \neq 0$, and different dynamical objects appear. Let us study the global dynamics of the CP problem when $K > 0$.

6.2 Introduction to global dynamics for $K > 0$

At this moment we are interested in knowing how the dynamics of the CP problem evolves when the parameter increases, we want to get an idea of the different dynamical aspects that one can have in our problem. We are going to focus our attention to the case $K = 0.0015749$ with $h = -1.7 < h_1$. Thanks to Figure 6.3 we know that the shape of the forbidden region of motion depends on the value of h, so the general aspect of the PSP also depends on the taken value of the energy. As now we only want to study possible dynamical phenomena that we can find in the CP, we are going to introduce only the case $h < h_1$, postponing other cases up to the next chapter.

Since the Hamiltonian (1.7) is non-integrable, when $K > 0$ the dynamics is richer and there appear other invariant objects typically expected in Hamiltonian systems with 2 degrees of freedom. Have a look to Figure 6.7.

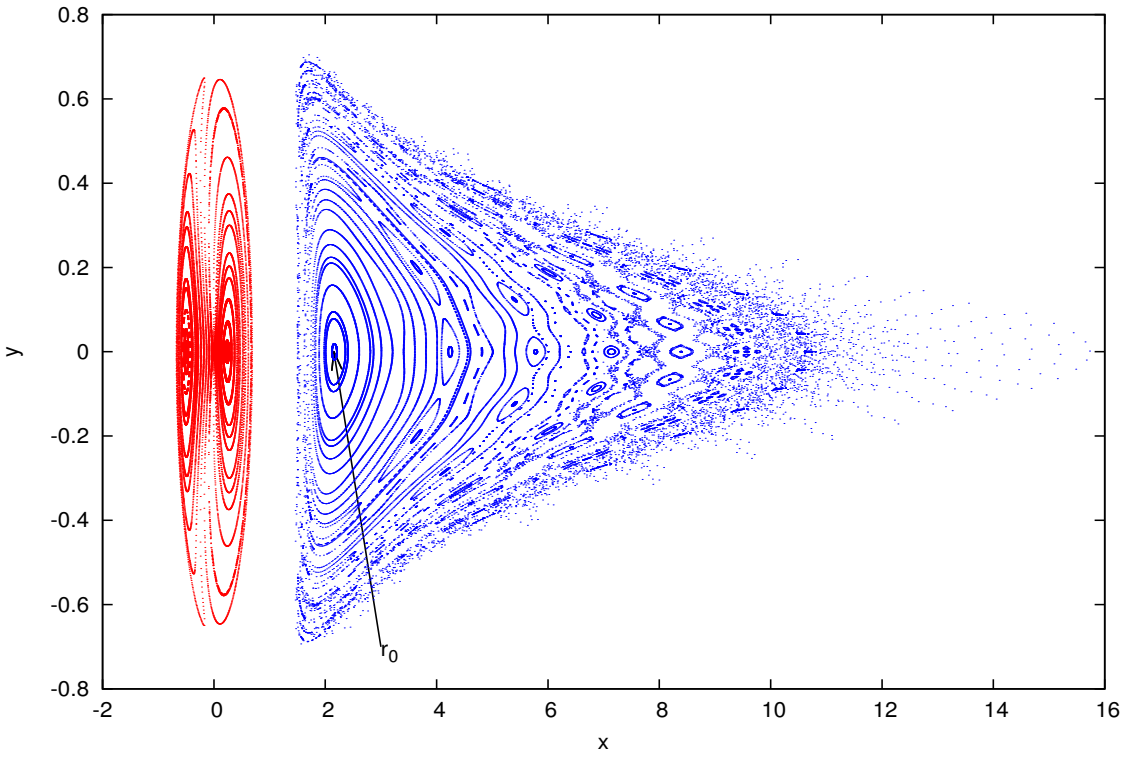

Figure 6.7: PSP when $K = 0.0015749$ and $h = -1.7 < h_1$. Points (x, y) on Σ. The movement in the inner component of motion has been plotted in red, while in the unbounded component of motion the behaviour appears in blue.

In order to study in more detail the bounded component of motion, observe Figure 6.8. In this case, as in Figure 6.4, the forbidden Hill's region is a ring whose boundaries are two closed curves (see left hand side of first row of Figure 3.1). As in Figure 6.4 we clearly see two fixed points in the bounded Hill's region of motion around the origin, which correspond to two periodic orbits, and we can appreciate invariant curves surrounding them. So when $K = 0$ there exist periodic orbits that remain also when $K > 0$.

6.2.1 Remark The arrows in Fig. 6.7-6.8 are related with some concepts that will be introduced in chapter 7. We are not going to introduce this notation now, but we want to prepare these figures in order to get results from them in the following sections.

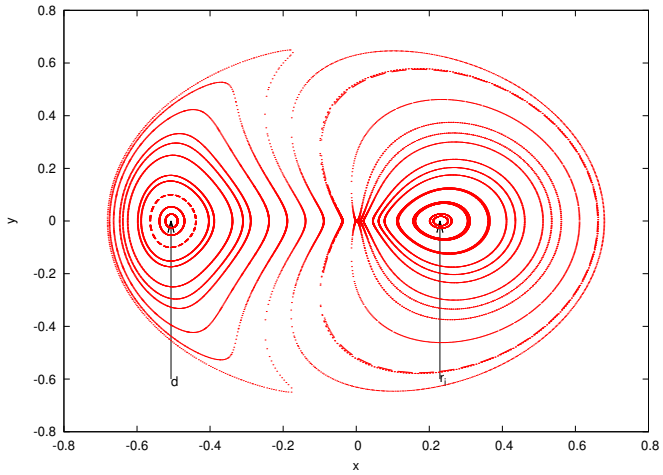

Figure 6.8: Bounded component of motion of Figure 6.7.

Observe that, for $K > 0$ the PSP keeps its inverted bell shape. As in $K = 0$, on the unbounded Hill's component we can see a fixed point and invariant curves surrounding it. The dynamics on this component of motion when $K \neq 0$ is not so regular due to the destruction of some of the invariant curves from $K = 0$ to $K > 0$. There are many periodic orbits (the three marked fixed points using arrows are the principal ones, but there are others!), quasiperiodic orbits (invariant curves surrounding fixed points), island chains and chaotic orbits. Let us study how an orbit on an island chain behaves.

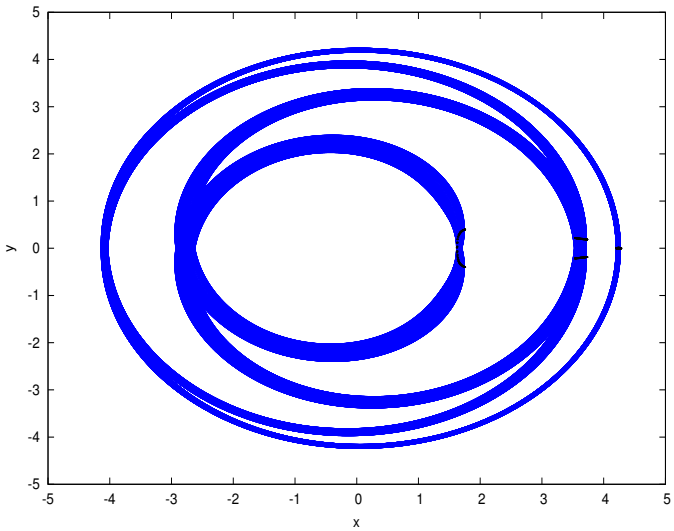

Figure 6.9: Orbit with an initial condition on an island ($x_0 = 4.2$, $y_0 = 0$, $x_0' = 0$, $y_0' < 0$). In black: (x, y) projection on the PSP. In blue: whole orbit.

As we can see, the orbits of points on an island move from island to island following the chain. The orbits starting in a chaotic region move without any pattern, the behaviour is difficult to describe. See Figure 6.10.

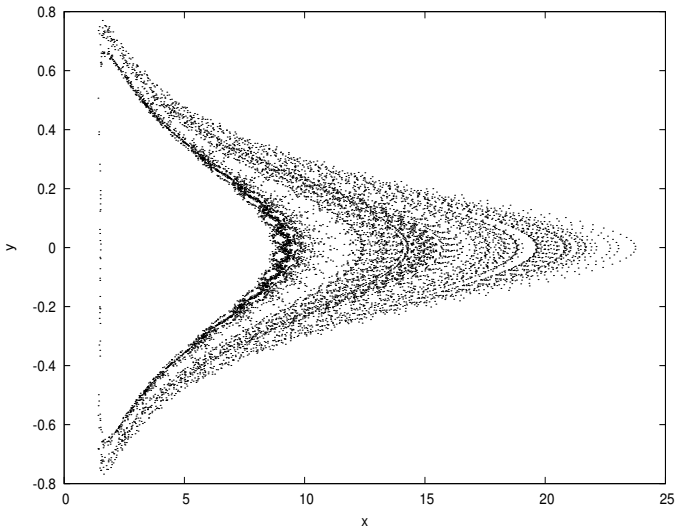

Figure 6.10: Chaotic motion. (x, y) projection on the PSP for the orbit $x_0 = 9$, $y_0 = 0$, $x_0' = 0$, $y_0' < 0$.

7
Periodic orbits

In order to construct the structure of our dynamical system we need to study other type of solutions: the ones which are periodic. Let $\phi_t(\xi)$ be a periodic solution of system (1.8)-(1.11). A cross-section to the periodic solution, or simply a section, is a hyperplane Σ of codimension one through ξ and transverse to

$$\mathbf{f}(\xi) = (f_1(\xi), f_2(\xi), f_3(\xi), f_4(\xi)).$$

If the solution starts on the section, by definition of periodic solution, after a time T it returns to Σ. Defining a Poincaré map $\mathbf{P}$ over Σ, $\mathbf{P}(\xi) = \xi$ and, consequently, the periodic solution $\phi_t(\xi)$ appears as a fixed point of $\mathbf{P}$.

Thanks to the previous reasoning, we can say that a fixed point of a Poincaré map is identified with a periodic orbit (PO) which passes through the taken Poincaré section, and this idea will be useful in the implementation of these kinds of orbits.

7.0.2 Definition A PO is called *direct* if its projection (x, y) moves anticlockwise. In the same way, a PO is called *retrograde* if the movement is clockwise.

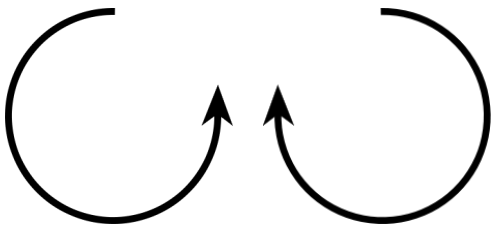

Figure 7.1: (x, y) projection. Left: Direct motion. Right: Retrograde motion.

Theory of stability (II)

Consider a discrete dynamical system given by a diffeomorphism $\mathbf{F}$,

$$\mathbf{x} \longmapsto \mathbf{F}(\mathbf{x}), \tag{7.1}$$

$\mathbf{x} \in \mathcal{U} \subset \mathbb{R}^n$, with a fixed point $\mathbf{p}$ ($\mathbf{F}(\mathbf{p}) = \mathbf{p}$). This fixed point can be classified in the following way:

7.0.3 Definition If all the eigenvalues of $\mathbf{A} := \mathbf{Df}(\mathbf{p})$ have modulus different from 1, then $\mathbf{p}$ is called *hyperbolic*.

7.0.4 Definition If all the eigenvalues of $\mathbf{A}$ have modulus equal to 1 and the Jordan associated matrix is diagonal, then $\mathbf{p}$ is called *elliptic*.

7.0.5 Theorem ***(Stability of fixed points)*** *Consider the discrete dynamical system (7.1) and its equilibrium point* $\mathbf{p}$*. Then,*

1) If all the eigenvalues of $\mathbf{A}$ *have modulus less than* 1*, then* $\mathbf{p}$ *is asymptotically stable.*

2) If there exists an eigenvalue of $\mathbf{A}$ *with modulus bigger than* 1*, then* $\mathbf{p}$ *is unstable.*

7.0.6 Remark As happens in the case of flows, we associate hyperbolic fixed points to instability, while the elliptic fixed points are associated to linear stability (although the 'nonlinear' stability of an elliptic point may become a difficult issue to prove).

7.0.7 Remark An initial condition ξ of a periodic orbit of period T can be regarded as a fixed point of the map $\mathbf{F} = \phi_T$.

Thanks to remark (7.0.7) and using theorem (7.0.5) one can talk about the stability of PO (see definition (1.1.7)) only considering $\mathbf{DF}(\xi) = \mathbf{D}\phi_T(\xi)$ and its eigenvalues.

7.0.8 Remark Observe that $\mathbf{D}\phi_T(\xi)$ is the monodromy matrix of system (1.8)-(1.11), which, for simplicity, will be called $\mathbf{M}$.

7.0.9 Lemma *Assume a Hamiltonian system of* n *degrees of freedom (*$2n$ *ODE). It is known that*

1) 1 *is an eigenvalue of* $\mathbf{M} = \mathbf{D}\phi_T(\xi)$ *of multiplicity* 2*.*

2) If λ *is an eigenvalue of* $\mathbf{M}$*, then* $\bar{\lambda}$*,* $\frac{1}{\lambda}$*,* $\frac{1}{\bar{\lambda}}$ *are eigenvalues of* $\mathbf{M}$*.*

Proof: See [2].

7.0.10 Corollary *Applying lemma (7.0.9) to our system, which has* 2 *degrees of freedom, we observe that*

$$Spec\ \mathbf{M} \quad = \quad \left\{1, 1, \lambda, \frac{1}{\lambda}\right\}. \tag{7.2}$$

Proof: Suppose λ eigenvalue of $\mathbf{M}$. Thanks to lemma (7.0.9) we only have two possibilities:

1) $\lambda \in \mathbb{R}$, so $\frac{1}{\lambda}$ is another eigenvalue of $\mathbf{M}$.

2) $\lambda \in \mathbb{C}$ with $\Im(\lambda) \neq 0$ and $|\lambda| = 1$. Let us study in more detail this second case.
Suppose $\lambda \in \mathbb{C}$ ($\Im(\lambda) \neq 0$) eigenvalue of $\mathbf{M}$, then $\bar{\lambda}$, $\frac{1}{\lambda}$ and $\frac{1}{\bar{\lambda}}$ are also eigenvalues. As $\lambda \neq \bar{\lambda}$, $\dim(\mathbf{M}) = 4$ and $\frac{1}{\lambda}$ can be rewritten as follows

$$\frac{1}{\lambda} = \frac{1}{\lambda}\frac{\bar{\lambda}}{\bar{\lambda}} = \frac{\bar{\lambda}}{|\lambda|^2},$$

the modulus of λ has to be equal to 1, otherwise we would have a number of eigenvalues bigger than the dimension of the matrix. In the same way,

$$\frac{1}{\bar{\lambda}} = \frac{1}{\bar{\lambda}}\frac{\lambda}{\lambda} = \frac{\lambda}{|\lambda|^2}.$$

Therefore

$$Spec\ \mathbf{M} = \left\{1, 1, \lambda, \frac{1}{\lambda}\right\}.$$

□

Our main interest now is to study the linear stability of a periodic orbit of our system restricted to the energy level $\mathcal{H} = h$. Thanks to corollary (7.0.10), we have that the characteristic polynomial of $\mathbf{M}$ is

$$p_c(s) = (s-1)^2(s-\lambda)\left(s - \frac{1}{\lambda}\right) = (s-1)^2\left(s^2 - \left(\lambda + \frac{1}{\lambda}\right)s + 1\right). \tag{7.3}$$

7.0.11 Definition $\left(\lambda + \frac{1}{\lambda}\right)$ is called the *stability parameter* and, for simplicity, we will denote it as k.

Observe that

$$k = \lambda + \frac{1}{\lambda} = tr\ \mathbf{M} - 2,$$

due to the fact that $tr\ \mathbf{M} = 2 + \lambda + \frac{1}{\lambda}$. So, we equal (7.3) to 0 and solve

$$s^2 - ks + 1 = 0. \tag{7.4}$$

The roots of (7.4) are

$$s_\pm = \frac{k \pm \sqrt{k^2 - 4}}{2},$$

being $s_+ = \lambda$ and $s_- = \frac{1}{\lambda}$. Let us call $\Delta = k^2 - 4$:

- If $k \in (-2, 2)$, then $\Delta < 0$ and

  $$\frac{k \pm i\sqrt{4 - k^2}}{2} = \begin{cases} \lambda \\ \frac{1}{\lambda}, \end{cases}$$

  so, using 2) of the proof of corollary (7.0.10),

  $$|\lambda| = \left|\frac{1}{\lambda}\right| = \sqrt{\frac{k^2}{4} + \frac{4 - k^2}{4}} = 1,$$

  and, consequently, we are in front of a elliptic (stable) orbit.

- If $k = -2$ or $k = 2$, then $\lambda = \frac{1}{\lambda} = 1$ or $\lambda = \frac{1}{\lambda} = -1$, respectively. Therefore, we are in front of a critical orbit.

- If $k \notin [-2, 2]$, then $\lambda,\ \frac{1}{\lambda} \in \mathbb{R}$. Moreover,

  $$\left.\begin{matrix} \lambda \\ \frac{1}{\lambda} \end{matrix}\right\} = \frac{k}{2} \pm \sqrt{\frac{k^2}{4} - 1},$$

  and

  $$\frac{k}{2} \pm \sqrt{\frac{k^2}{4} - 1} \neq \pm 1,$$

  so $|\lambda|,\ \left|\frac{1}{\lambda}\right| \neq 1$. Then there exists one eigenvalue with modulus bigger than 1 and another one with modulus smaller than 1, and consequently we have a hyperbolic (unstable) orbit (see theorem (7.0.5)).

Summarizing, if we want to study the stability of a PO, we only have to study the eigenvalues of its monodromy matrix and use the exposed classification. This classification will be implemented as an external function of the method of computation of PO that is going to be introduced in the next section.

7.1 Implementation of PO

The main goal of this section is to find periodic orbits numerically. Given a cross-section $\Sigma = \{\mathbf{x} : g(\mathbf{x}) = 0\}$, we want to obtain a periodic orbit passing through Σ with energy level h. In other words, we are looking for $h \in \mathbb{R}$, $T \in \mathbb{R}_+$ and $\mathbf{x} \in \Sigma$ such that

$$\begin{cases} \mathcal{H}(\mathbf{x}) - h = 0 \\ g(\mathbf{x}) = 0 \\ \phi_T(\mathbf{x}) - \mathbf{x} = \mathbf{0} \end{cases} \Leftrightarrow G(\mathbf{Z}) = 0 \text{ with } \mathbf{Z} = \begin{pmatrix} h \\ T \\ \mathbf{x} \end{pmatrix}. \tag{7.5}$$

It is clear that a solution h, T, $\mathbf{x}$ of this system corresponds to a PO of period T such that $\mathcal{H}(\mathbf{x}) = h$.

Our aim now is to solve (7.5). In order to do this, we fix h, so the variables now are T and $\mathbf{x}$. Then,

$$\begin{aligned} \text{Number of equations} &: 1 + 1 + 4 = 6, \\ \text{Number of variables} &: 1 + 4 = 5, \end{aligned}$$

and, consequently, we are in front of an overdetermined system.

7.1.1 Remark Fixing h, we are capable of finding periodic orbits on a given Poincaré section with a known energy level. It means that, thanks to this implementation, we will be able to obtain numerically the fixed points of PSP figures.

Let us consider system (7.5) in short notation,

$$G(\mathbf{Z}) = 0 \Leftrightarrow \begin{pmatrix} \mathcal{H}(\mathbf{x}) - h \\ g(\mathbf{x}) \\ \phi_T(\mathbf{x}) - \mathbf{x} \end{pmatrix} = \begin{pmatrix} 0 \\ 0 \\ \mathbf{0} \end{pmatrix}, \tag{7.6}$$

and assume that

$$g(\mathbf{x}) = 0 \Leftrightarrow c_1 x + c_2 y + c_3 p_x + c_4 p_y = 0. \tag{7.7}$$

Observe that

$$\mathbf{DG}(\mathbf{Z}) = \begin{pmatrix} -1 & 0 & \frac{\partial \mathcal{H}}{\partial x} & \frac{\partial \mathcal{H}}{\partial y} & \frac{\partial \mathcal{H}}{\partial p_x} & \frac{\partial \mathcal{H}}{\partial p_y} \\ 0 & 0 & c_1 & c_2 & c_3 & c_4 \\ 0 & f_1(\phi_T(\mathbf{x})) & \frac{\partial \phi_1}{\partial x}\Big|_{t=T} - 1 & \frac{\partial \phi_1}{\partial y}\Big|_{t=T} & \frac{\partial \phi_1}{\partial p_x}\Big|_{t=T} & \frac{\partial \phi_1}{\partial p_y}\Big|_{t=T} \\ 0 & f_2(\phi_T(\mathbf{x})) & \frac{\partial \phi_2}{\partial x}\Big|_{t=T} & \frac{\partial \phi_2}{\partial y}\Big|_{t=T} - 1 & \frac{\partial \phi_2}{\partial p_x}\Big|_{t=T} & \frac{\partial \phi_2}{\partial p_y}\Big|_{t=T} \\ 0 & f_3(\phi_T(\mathbf{x})) & \frac{\partial \phi_3}{\partial x}\Big|_{t=T} & \frac{\partial \phi_3}{\partial y}\Big|_{t=T} & \frac{\partial \phi_3}{\partial p_x}\Big|_{t=T} - 1 & \frac{\partial \phi_3}{\partial p_y}\Big|_{t=T} \\ 0 & f_4(\phi_T(\mathbf{x})) & \frac{\partial \phi_4}{\partial x}\Big|_{t=T} & \frac{\partial \phi_4}{\partial y}\Big|_{t=T} & \frac{\partial \phi_4}{\partial p_x}\Big|_{t=T} & \frac{\partial \phi_4}{\partial p_y}\Big|_{t=T} - 1 \end{pmatrix}, \tag{7.8}$$

is a 6×6 matrix. But, since we have fixed h, in order to solve system (7.5) we apply Newton's method to this system with 6 equations and variables T, x,y,p_x,p_y. So, the differential of our problem is not exactly $\mathbf{DG}(\mathbf{Z})$, we consider $\overline{\mathbf{DG}}$ such that

$$\mathbf{DG} = \left(\;\middle|\; \overline{\mathbf{DG}} \right), \tag{7.9}$$

where we skip the first column of $\mathbf{DG}$, which corresponds to the partial derivatives with respect to h.

Now take an initial seed $\mathbf{Z}^{(0)}$ for Newton's method such that

$$\mathbf{Z}^{(0)} = \begin{pmatrix} h \\ T^{(0)} \\ x^{(0)} \\ y^{(0)} \\ p_x^{(0)} \\ p_y^{(0)} \end{pmatrix},$$

where the first component will remain fixed during all the process because h is given. In fact, we can take an initial seed considering only the variables that we want to approximate,

$$\mathbf{y}^{(0)} = \begin{pmatrix} T^{(0)} \\ x^{(0)} \\ y^{(0)} \\ p_x^{(0)} \\ p_y^{(0)} \end{pmatrix}.$$

Then we only need to follow the typical steps which define Newton's method:

1) Compute $\mathbf{G}(\mathbf{Z}^{(0)})$. If $||\mathbf{G}(\mathbf{Z}^{(0)})|| < \text{TOL}$ (typically, TOL$= 10^{-13}$), we can stop and consider that $\mathbf{Z}^{(0)}$ is solution of system (7.5). Otherwise, go to step 2.

2) Look for

$$\Delta\mathbf{y}^{(0)} = \begin{pmatrix} \Delta T^{(0)} \\ \Delta x^{(0)} \\ \Delta y^{(0)} \\ \Delta p_x^{(0)} \\ \Delta p_y^{(0)} \end{pmatrix}$$

such that

$$\overline{\mathbf{DG}}(\mathbf{y}^{(0)})\Delta\mathbf{y}^{(0)} = -\mathbf{G}(\mathbf{Z}^{(0)}). \tag{7.10}$$

7.1.2 Remark In order to solve the overdetermined linear system (7.10), we apply a least-squares method. In our case, we have used the linear algebra library Eigen for implementations in C++ language.

Once we have $\Delta\mathbf{y}^{(0)}$, we take

$$\mathbf{Z}^{(1)} = \mathbf{Z}^{(0)} + \begin{pmatrix} 0 \\ \Delta T^{(0)} \\ \Delta x^{(0)} \\ \Delta y^{(0)} \\ \Delta p_x^{(0)} \\ \Delta p_y^{(0)} \end{pmatrix}.$$

3) Go to 1 with $\mathbf{Z}^{(1)} \to \mathbf{Z}^{(0)}$.

In general, given $\mathbf{Z}^{(0)}$, we compute $\mathbf{y}^{(0)}$. Repeating the explained steps 1-3, we obtain the sequence

$$\mathbf{Z}^{(k)} = \begin{pmatrix} h \\ T^{(k)} \\ x^{(k)} \\ y^{(k)} \\ p_x^{(k)} \\ p_y^{(k)} \end{pmatrix},$$

using that

$$\mathbf{Z}^{(k+1)} = \mathbf{Z}^{(k)} + \Delta\mathbf{y}^{(k)} = \mathbf{Z}^{(k)} + \begin{pmatrix} 0 \\ \Delta T^{(k)} \\ \Delta x^{(k)} \\ \Delta y^{(k)} \\ \Delta p_x^{(k)} \\ \Delta p_y^{(k)} \end{pmatrix},$$

where

$$\overline{\mathbf{DG}}(\mathbf{y}^{(k)})\Delta\mathbf{y}^{(k)} = -\mathbf{G}(\mathbf{Z}^{(k)}).$$

So we expect

$$\lim_{k\to+\infty} \mathbf{Z}^{(k)} = \mathbf{Z} = \begin{pmatrix} h \\ \mathbf{y} \end{pmatrix} = \begin{pmatrix} h \\ T \\ x \\ y \\ p_x \\ p_y \end{pmatrix},$$

being x, y, p_x, p_y the wanted initial condition of a periodic orbit, with period T and energy level h.

7.1.3 Remark Given a value of h, system (7.5) maybe does not have a unique solution T, x, y, p_x, p_y. The output solution of our implementation depends on the initial seed given in Newton's method. As we know, to ensure the convergence of Newton's method we need an initial seed close enough to the desired solution.

7.1.4 Remark There are other possible ways of implementation of periodic orbits, we could compute only symmetric periodic orbits given the cross-section $g(\mathbf{x}) = y = 0$ by using *bisection method*'s idea:

1) Assume a given K and a fixed level of energy h. Implement a routine such that, given an initial x, sign of y' and h, computes (as output) y'. Then consider the initial condition $(x, 0, 0, y')$.

2) Given the initial condition computed in 1), implement a routine such that returns as output $F(x) = x'$ at a given crossing.

3) Vary x such that you find x_1 and x_2 in such a way that, given the initial conditions $(x_1, 0, 0, y_1')$ and $(x_2, 0, 0, y_2')$ from 1), $F(x)$ changes sign.

4) Once you have 3), refine x, using a method to find zeros of equations (for example, bisection method), in such a way that $F(x) = 0$ (i.e. $|F(x)| < \mathrm{TOL}$). Thanks to the symmetry of the problem, the initial condition $(x, 0, 0, y')$ describes a symmetric periodic orbit with respect $y = 0$.

Observe that this method has the restriction of the cross-section, while with the other one any section can be taken. We have implemented both methods, but we are going to use the results from the first one.

	x	y	p_x	p_y
d	−0.507009435199939	0	0	−1.403310339431121
$\mathbf{r_i}$	0.229690715908056	0	0	−2.085346092561523
$\mathbf{r_o}$	2.155292149997760	0	0	0.683407657912759

Table 7.1: Initial conditions for the main families of symmetric periodic orbits shown in the PSP for $K = 0.0015749$ and $h = -1.7$. See Fig. 6.7-6.8.

7.2 Continuation of families of PO

It is well-known that a lot of dynamical objects are preserved by continuation when the parameter of the dynamical system changes. This intuitive idea gives us some information about what kind of behaviour we can have after a small modification of the parameter, taking into consideration the dynamical aspects of the system without any modification of the parameter. In this section we want to study families of periodic orbits obtained by varying the level of energy h from the initial case seen in Fig. 6.7-6.8, in other words, we would like to know how a periodic orbit of Figure 6.7 evolves when the energy level of the system increases or decreases.

Figure 6.7 (and Fig. 6.8) mainly shows three fixed points (amongst others with less importance in our study), which correspond to the three periodic orbits whose continuation we want to study. On the left hand side component of Figure 6.7 we clearly see two fixed points (observe Fig. 6.8), the one with $x_0 < 0$ corresponds to a direct periodic orbit of family d, while the one with $x_0 > 0$ represents a retrograde periodic orbit of family r_i. In the same way, on the right hand side of the same figure we can see the unbounded Hill's component, where a retrograde periodic orbit of family r_o is identified. The three fixed points coincide in the fact that each periodic orbit is symmetric, so we are going to explore the existence of some families of symmetric periodic orbits.

7.2.1 Remark The names of the families of PO are related to the characterization of each orbit. See the following descriptions:

- d is a family of direct periodic orbits.
- r_i is a family of retrograde periodic orbits located in the inner region of motion.
- r_o is a family of retrograde periodic orbits located in the outer region of motion.

Using the implementation presented at the beginning of section 7.1, we are able to find the exact position of the three commented fixed points of Figure 6.7, and thanks to this we can obtain an initial condition for each one of the three associated periodic orbits. These initial conditions will be useful for the continuation of the families, and for this reason they can be seen in Table 7.1.

Now we proceed to do the continuation of the three introduced families of periodic orbits (see the following three sections). All the explanations are done for $K = 0.0015749$ (which corresponds to the value of K of Figure 6.7). For this value of K we obtain $x_1 = -0.9994753080$, $h_1 = -1.5015744867596$; $x_2 = 1.00052524235$, $h_2 = -1.498424686470$.

7.2.2 Notation We denote by

- x_0 the value of the x-coordinate of an initial condition of a PO (typically x_0, $y_0 = 0$, $x_0' = 0$, y_0').

- x_{hp} the value of the x-coordinate of a PO at half period.
- T the period of a PO.
- h the energy (or the value of the hamiltonian) of a PO.
- α the stability parameter.

7.2.3 Remark In our case, you can start the continuation at $h = -1.7$ taking as initial periodic orbits the ones shown in Table 7.1.

7.2.1 Family of direct PO

We can continue the family d. The output of our code is projected in Figure 7.2, which helps us to understand the behaviour of the family. Let us comment the properties of d:

1) The family exists for $h \in (-\infty, h_1)$. There are two limiting periodic orbits: the origin, seen as an 'equilibrium point' (period ≈ 0), for $h \to -\infty$ and a periodic orbit of *infinite* period, that tends to the invariant manifolds of $\mathcal{L}_1$ when $h \to h_1$. We can see in Figure 7.2 how the value of y' tends to 0 as $h \to h_1$.

2) The orbits are always (linearly) stable with infinitely many critical orbits (that is, with α equal to 2 or -2).

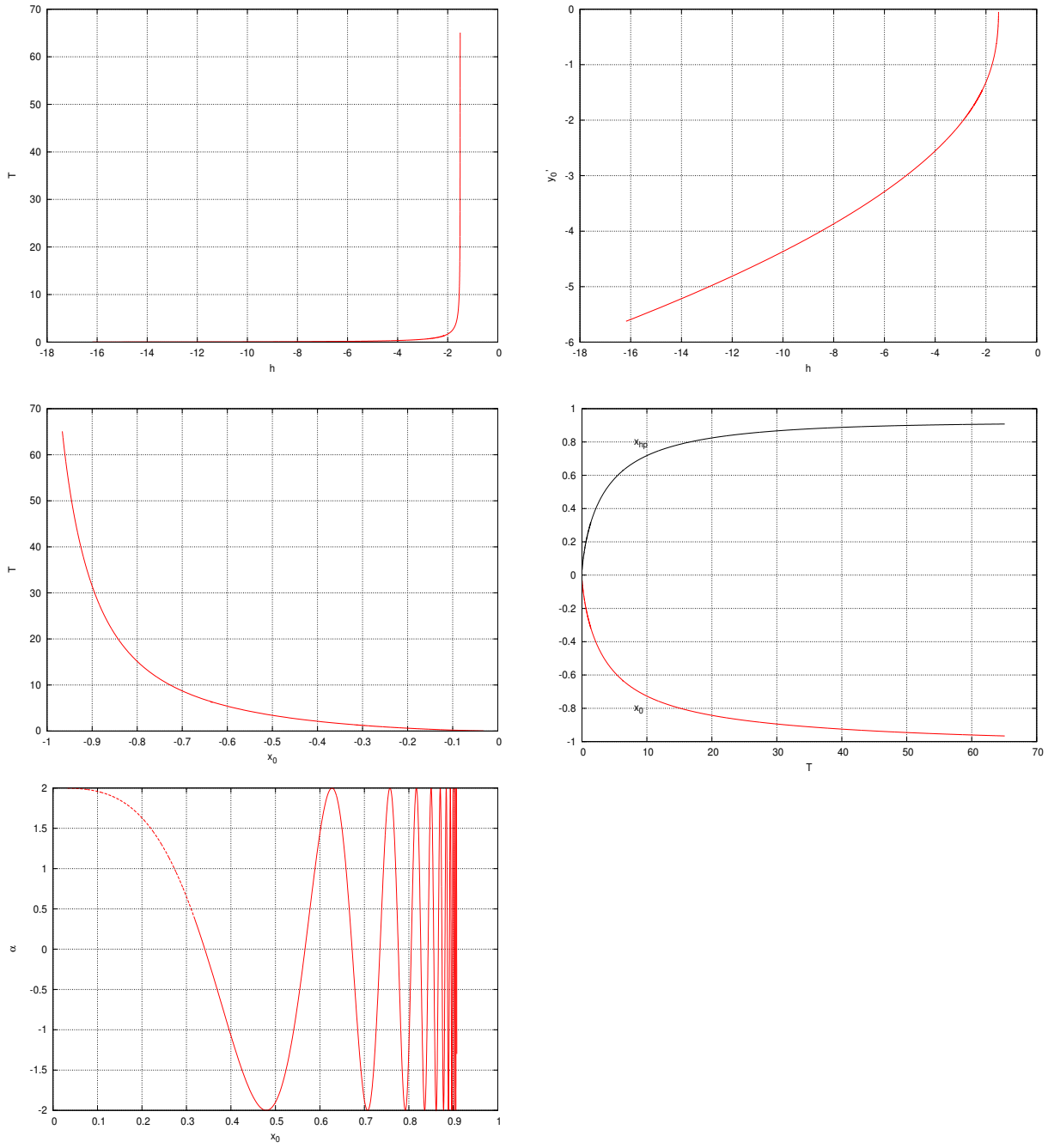

Figure 7.2: Information about the continuation of the family d.

7.2.2 Family of internal retrograde PO

Using our implementation to continue the family r_i, we obtain the following plots:

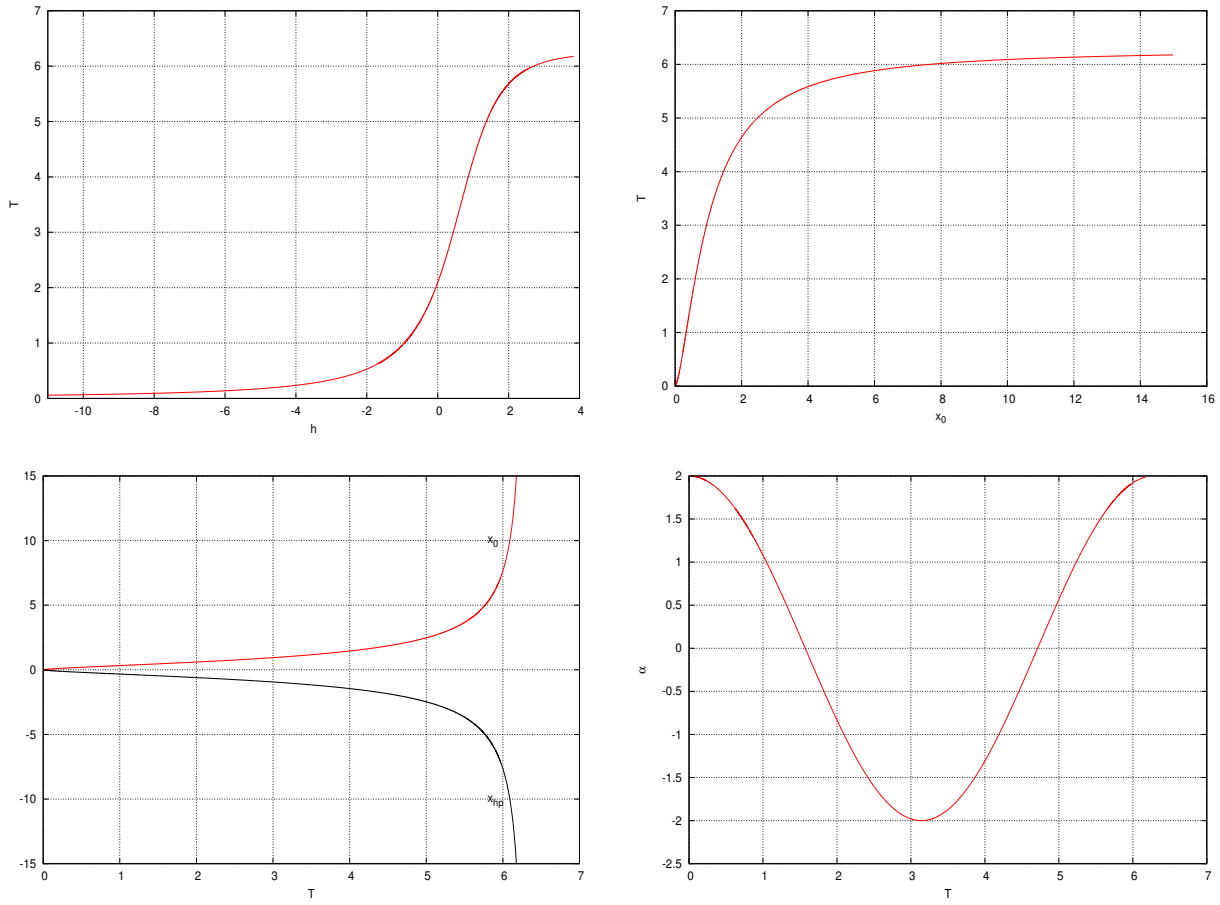

Figure 7.3: Information about the continuation of the family r_i.

Thanks to Figure 7.3 we observe that the internal retrograde family of PO identified in Figure 6.8 has the following properties:

1) The family exists for all values of the energy (both positive and negative).

2) Along the family, the period belongs to $[0, 2\pi]$. There are two limiting periodic orbits: one of *infinite* radius and period 2π when $h \to +\infty$, and an 'equilibrium point' for $h \to -\infty$ at $x_0 = y_0 = 0$.

3) The orbits are always (linearly) stable. There is a tangency with $\alpha = -2$ for $h \approx 0.5$ and $x_0 \approx 0.998$.

7.2.3 Family of external retrograde PO

Applying our implementation to the other retrograde family, we have the following output:

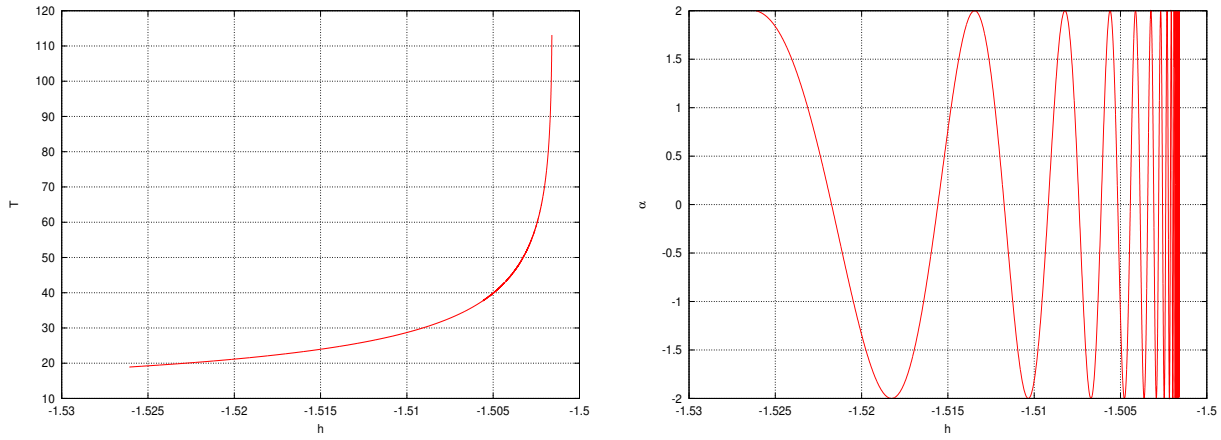

Figure 7.4: Information about the continuation of the family r_o.

Thanks to Figure 7.4 we observe that the family r_o has the following properties:

1) The family exists for $-\infty < h < h_1$. There appear many bifurcating families and, for this reason, the continuation is very complicated. The range of h in Figure 7.4 is very small due to the fact that at $h_* = -1.526$ there is a bifurcation and from there the main family is difficult to follow.

7.2.4 Lyapunov periodic orbits

Up to here we have presented three families of periodic orbits, the most important ones which were identified in Figure 6.7. In this section we want to study a different type of PO, the ones which are associated to the equilibrium points of our problem. To do it we apply the well-known Lyapunov center theorem.

7.2.4 Theorem *(**Lyapunov center theorem**) Consider a Hamiltonian system (or a system with a first integral)*

$$\dot{\mathbf{x}} = \mathbf{f}(\mathbf{x}),$$

being $\mathbf{f}$ *smooth enough in* $\mathcal{U} \subset \mathbb{R}^n$*, for* $\mathcal{U}$ *an open set. Suppose that the system has an equilibrium point* $\mathbf{x_0}$ *with characteristic exponents (i.e. eigenvalues of* $\mathbf{Df}(\mathbf{x_0})$*)* $\pm\omega i$*,* $\lambda_3,\ldots,\lambda_n$*, where* $i\omega \neq 0$ *is pure imaginary. If* $\frac{\lambda_j}{i\omega}$ *is never an integer for* $j = 3,\ldots,n$*, then there exists a one-parameter family of periodic orbits emanating from the equilibrium point. Moreover, when approaching the equilibrium point along the family, the periods tend to* $\frac{2\pi}{\omega}$ *and the nontrivial multipliers tend to* $\exp\left(\frac{2\pi\lambda_j}{\omega}\right)$*,* $j = 3,\ldots,n$*.*

Proof: See [2].

Applying theorem (7.2.4) to our problem, we can take $\mathbf{x_0} = \mathcal{L}_1$ or $\mathbf{x_0} = \mathcal{L}_2$. Let us see in more detail de following cases:

1) Suppose $\mathbf{x_0} = \mathcal{L}_1$. As we already know, $\mathcal{L}_1$ is of type center $\times$ saddle for $K > 0$, so

$$Spec\ \mathbf{Df}(\mathbf{x_0}) = \{\pm a, \pm bi\} \text{ with } a,\ b \neq 0.$$

By Lyapunov, as $\frac{a}{ib} \notin \mathbb{Z}$, there exists a one parameter family of PO, called *Lyapunov PO* (LPO), and the period of the PO (along the family) tends to $\frac{2\pi}{b}$ as the PO tends to $\mathbf{x_0}$. For simplicity this family will be called lo_1.

2) Now suppose $\mathbf{x_0} = \mathcal{L}_2$. As we already know, $\mathcal{L}_2$ is of type center $\times$ center for $K \leq \frac{3^{-4/3}}{2} = 0.11556021$, so

$$Spec\ \mathbf{Df}(\mathbf{x_0}) = \{\pm ai, \pm bi\} \text{ with } a,\ b \neq 0.$$

Suppose $a > b$. As we have two pairs of pure imaginary complex, first of all we take $\pm ai$. Observe that

$$\frac{bi}{ai} = \frac{b}{a} < 1 \Rightarrow \frac{bi}{ai} \notin \mathbb{Z},$$

then there exists a 1-parameter family of PO with period tending to $\frac{2\pi}{a}$ as the PO goes to $\mathbf{x_0}$. This family is called *short period family of PO* (written as lo_{2s}), due to the fact that $a > b$.

In the same way, taking $\pm bi$, we observe that

$$\frac{ai}{bi} = \frac{a}{b} > 1, \tag{7.11}$$

so, for a given value of the parameter K, we must check if $\frac{a}{b}$ is an integer number. If $\frac{a}{b} \notin \mathbb{Z}$ then there exists a second family of PO emanating from $\mathbf{x_0}$ with period tending to $\frac{2\pi}{b}$. This family is called *long period family of PO* (written as lo_{2l}), due to $b < a$.

7.2.5 Remark Suppose $K = 0.0015749$. Then

$$Spec\ \mathbf{Df}(\mathcal{L}_2) = \{\pm bi, \pm ai\} = \{\pm 0.068791054i, \pm 0.998419683i\},$$

being $a = 0.998419683$ and $b = 0.068791054$. As $\frac{a}{b} = 14.513801022 \notin \mathbb{Z}$, using the previous reasoning there exist two 1-parameter families of PO emanating from $\mathcal{L}_2$, one of short period and another one of long period. See Figure 7.5.

Now we are interested in computing the commented Lyapunov families when $K = 0.0015749$ (as before). In order to do it, we use the same implementation than for the continuation of d, r_i and r_o, now starting the continuation from the equilibrium point.

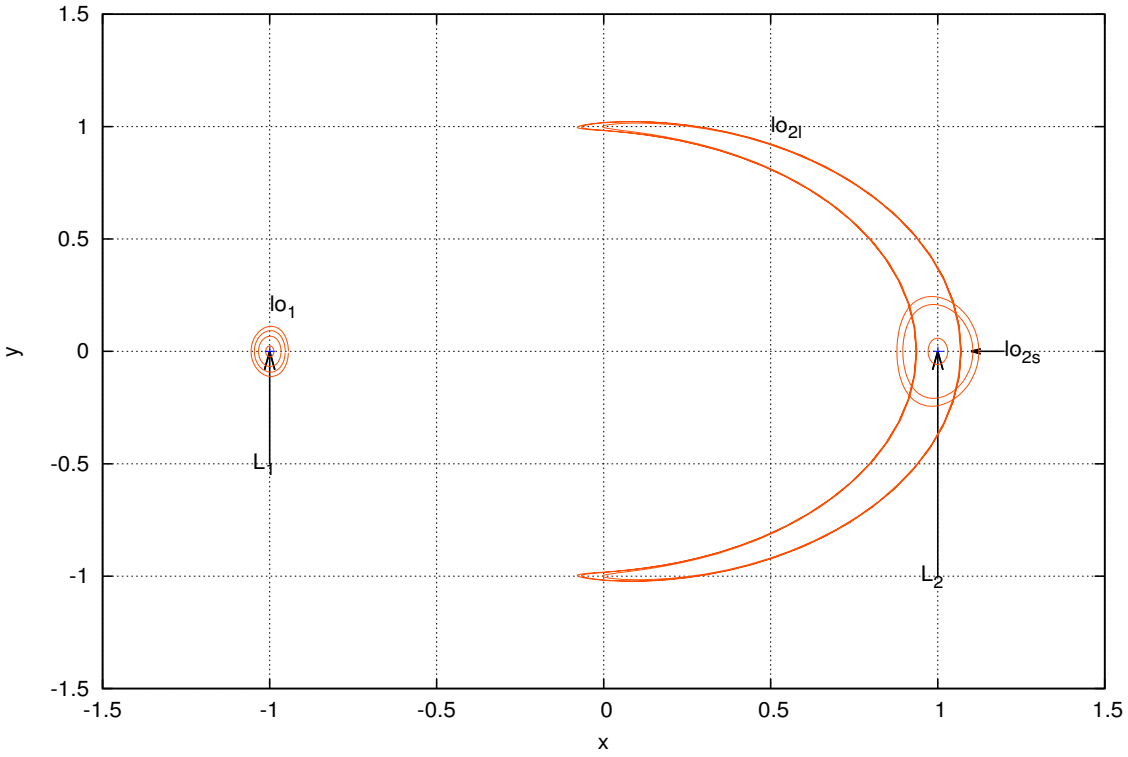

Figure 7.5: Intuitive idea of the families of Lyapunov PO when $K = 0.0015749$.

Family of LPO around $\mathcal{L}_1$

This family has the following properties (see Figure 7.6):

1) The family exists for $h \geq h_1$. The orbits computed are unstable.

2) We stop the continuation when the orbit is close to a collision with the origin, with a high level of difficulty to approach correctly the origin. We might continue the family using regularized coordinates.

3) As stated by Lyapunov theorem, $T_{po} \to \frac{2\pi}{b} = 6.27333$ as the PO approaches the equilibrium, where $\pm bi = \pm 1.00157i$ are eigenvalues of the Jacobian matrix at $\mathcal{L}_1$.

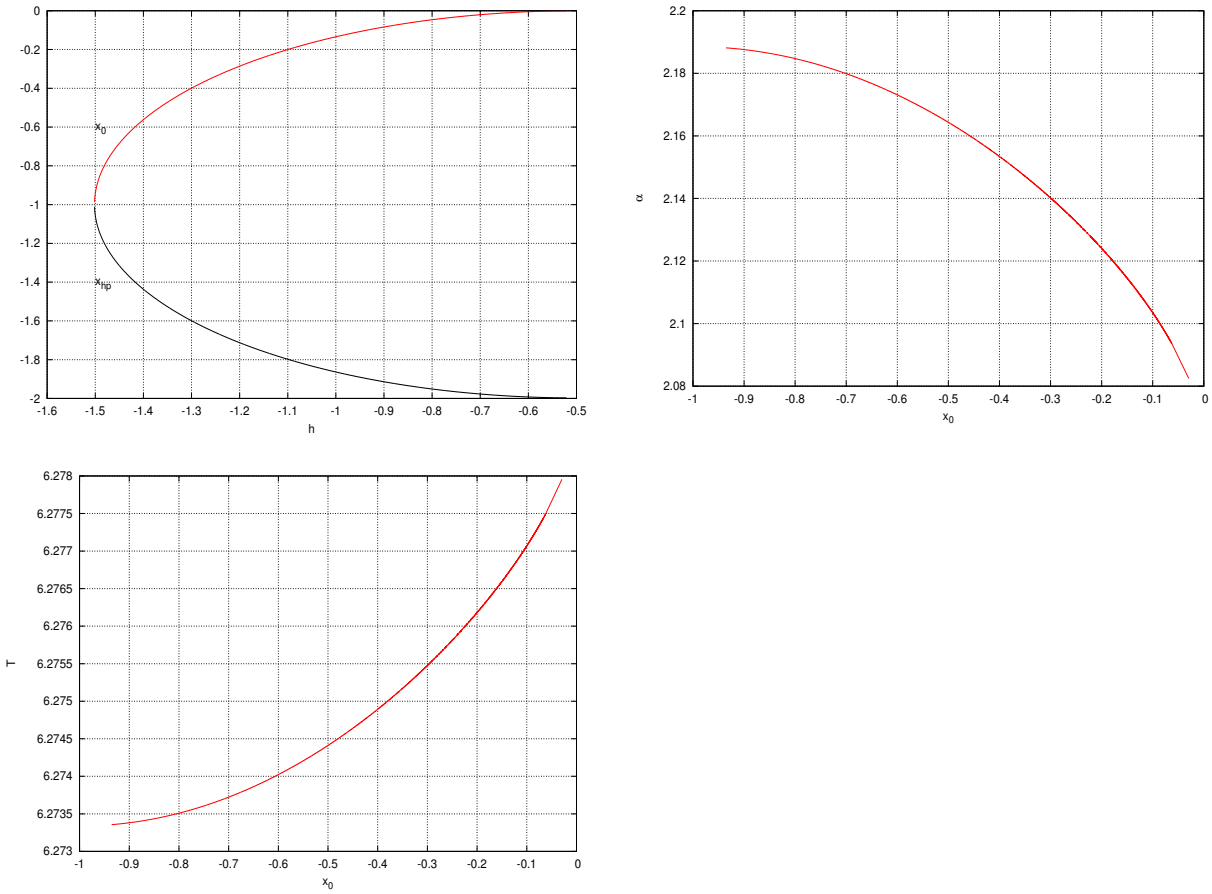

Figure 7.6: Information about the continuation of the family lo_1.

Family of LPO around $\mathcal{L}_2$

We distinguish here the two families of short and long period associated to $\mathcal{L}_2$, lo_{2s} and lo_{2l}, respectively.

Family of short period: lo_{2s}

The main properties of the studied family are deduced thanks to Figure 7.7:

1) The family exsits for $h \geq h_2$. The computed orbits are stable.

2) We stop the continuation when the orbit is close to a collision with the origin. We might continue the family using regularized coordinates.

3) As stated by Lyapunov theorem, $T_{po} \to \frac{2\pi}{a} = 6.29313$ as the PO approaches the equilibrium, where $\pm ai = \pm 0.99841i$ are eigenvalues of the Jacobian matrix at $\mathcal{L}_2$.

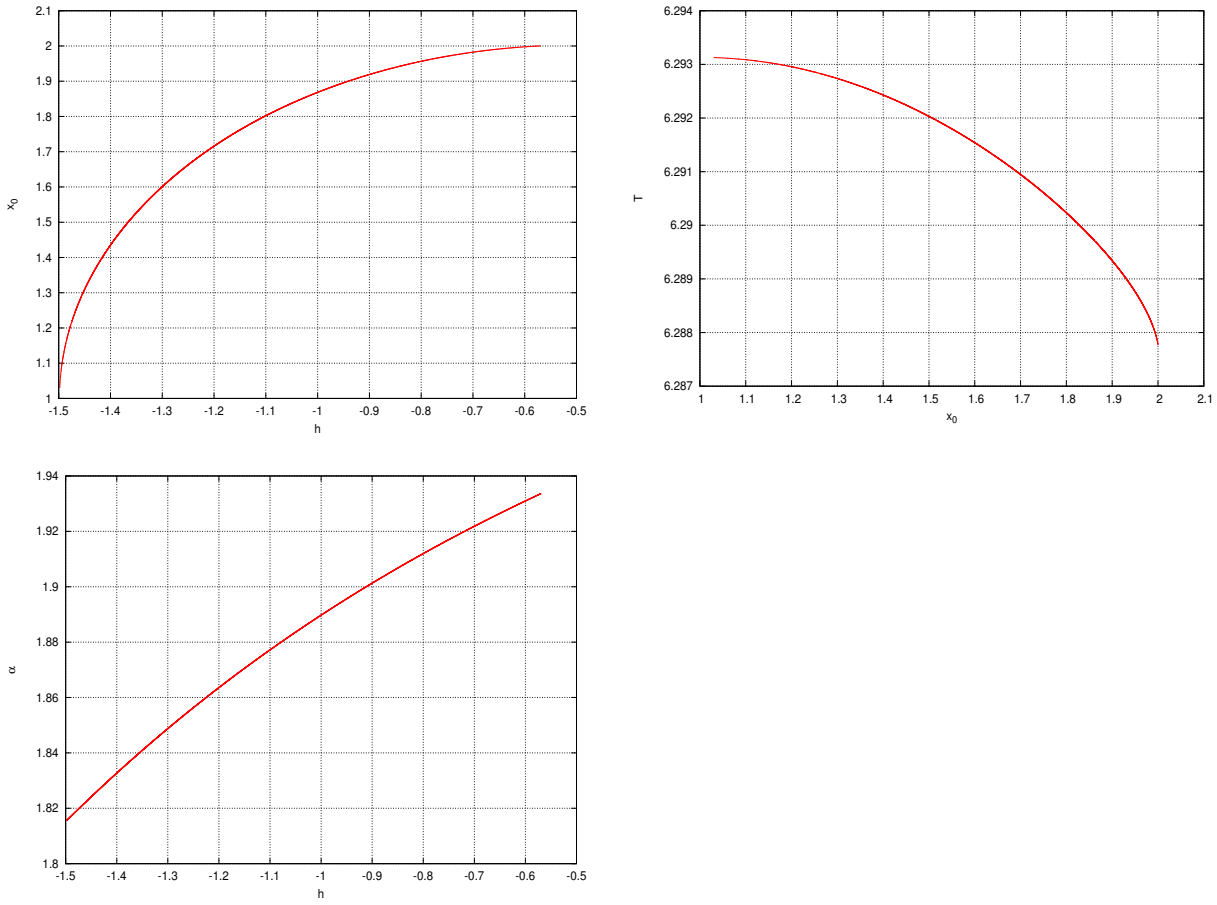

Figure 7.7: Information about the continuation of the family lo_{2s}.

Finally, we present the continuation of the long period family of LPO.

Family of long period: lo_{2l}

The main properties of lo_{2l} are deduced thanks to Figure 7.8:

1) The family exists for $h_1 \leq h \leq h_2$. The computed orbits are stable.

2) We stop the continuation when the energy tends either to h_1 or h_2.

3) As stated by Lyapunov theorem, when $h \to h_2$, $T_{po} \to \frac{2\pi}{b} = 91.33731$, where $\pm bi = \pm 0.06879i$ are eigenvalues of the Jacobian matrix at $\mathcal{L}_2$.

4) There are many bifurcations along the family.

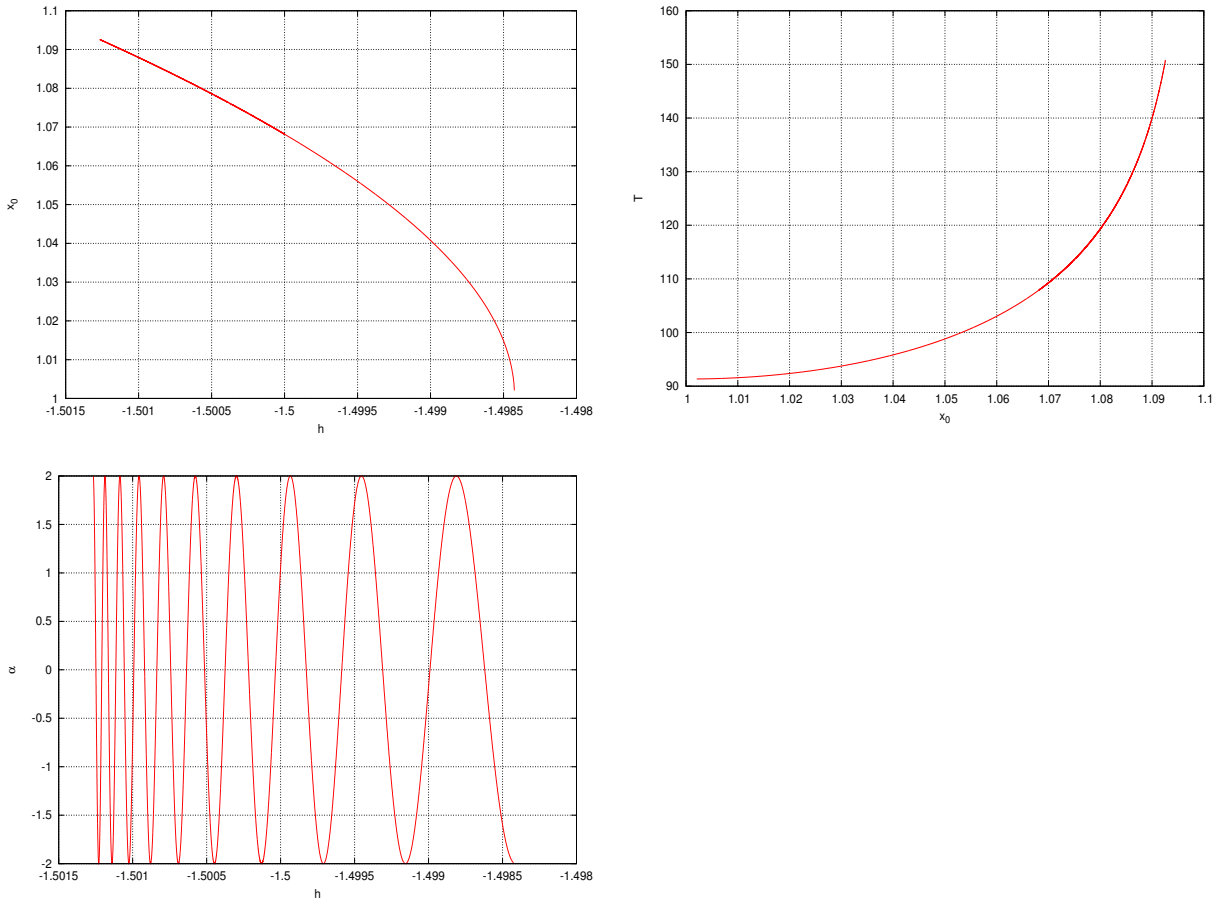

Figure 7.8: Information about the continuation of the family lo_{2l}.

7.3 Global dynamics for $K > 0$: coming back to PSP

In this section we would like to verify some of the obtained results about continuation of families of periodic orbits using the characterization of the Poincaré section plot when $K = 0.0015749$ and $h_1 < h < h_2$. For this range of energies the zvc is a bounded right-moon shaped curve that intersects the x-axis at two points (see Figure 7.9, where a PSP for $h = -1.5$ is shown). In this figure the forbidden region of motion is recognizable among the iterates of the Poincaré map in the inner region and those in the outer region. Recall that in this case there is a neck that allows trajectories travelling from the inner region (around the origin) to the outer region. Therefore there is no motion barrier (on the (x, y) position variables) around the origin.

When $h = h_1$ the equilibrium point $\mathcal{L}_1$ appears and, as we have seen in Fig. 7.2-7.4, the family of direct periodic orbits and the external family of retrograde periodic orbits, existing for $h < h_1$, disappear for $h = h_1$ tending to the 1-dimensional manifolds W^u and W^s of the unstable equilibrium point $\mathcal{L}_1$, as we explained some sections ago. Now, for each $h > h_1$, on one hand there exists the LPO around $\mathcal{L}_1$ and, on the other hand, there also exists the internal retrograde periodic orbit (and the invariant curves around

it) that persists for all values of the energy. And, although $\mathcal{L}_2$ does not exist, the LPO of long period of family lo_{2l} does. See again Figure 7.9 to observe the commented results.

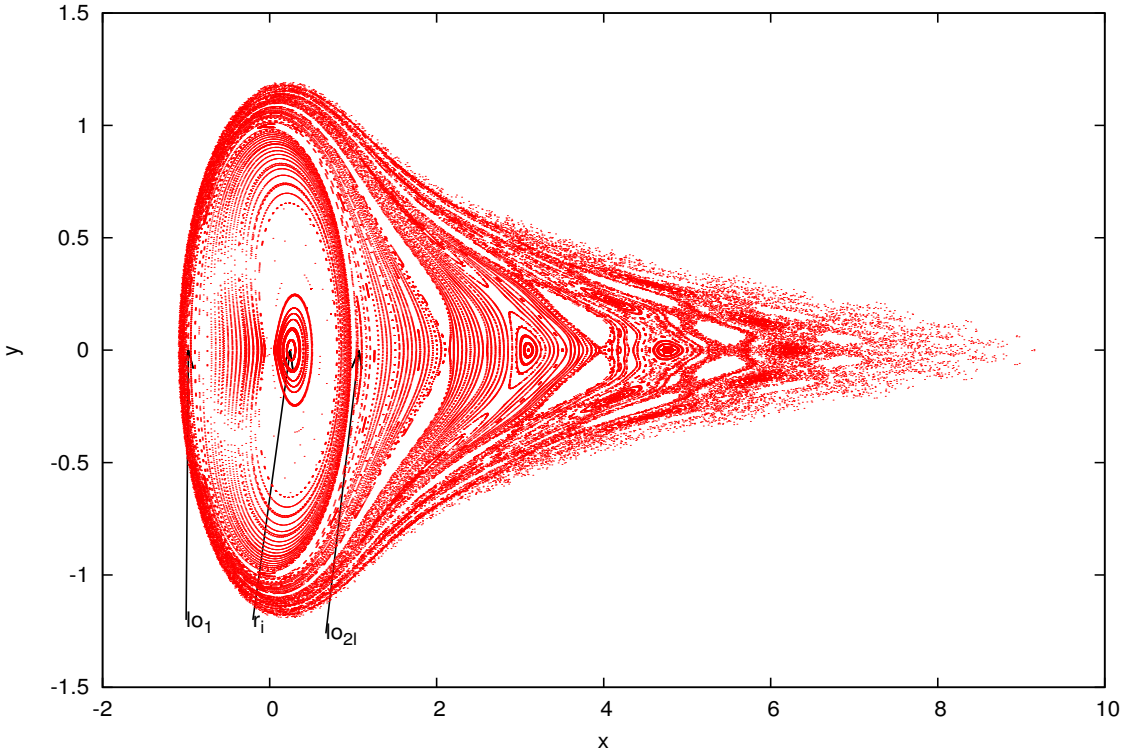

Figure 7.9: PSP when $K = 0.0015749$ and $h_1 < h < h_2$. The periodic orbits of the main families are shown.

Finally, observe that around the origin there is still a region of bounded orbits due to the persistence of some invariant curves that confine the motion inside them. Outside the outermost invariant curve around the origin (there are infinitely many other invariant curves farther on, grouped in chain of islands) the chaoticity increases.

8 Homoclinic connections to LPO

The purpose of this chapter is to give a first idea of the dynamics around the Lyapunov periodic orbits, by means of the behaviour of their invariant manifolds and the existence of homoclinic connections. At this point it is needed to introduce a theory similar to the one given at the beginning of chapter 4. For additional information see [2].

8.0.1 Definition Consider a ($\mathcal{C}^1$) diffeomorphism $\mathbf{F}$ (system (7.1)) and let $\mathbf{p}$ be a fixed point. Let $\varepsilon > 0$ be given, then the *local stable manifold* associated to $\mathbf{p}$ is

$$W^s(\varepsilon) = \{\mathbf{x} \in \mathbb{R}^n : |\mathbf{F}^k(\mathbf{x}) - \mathbf{p}| < \varepsilon \text{ for all } k \geq 0\}.$$

Similarly, the *local unstable manifold* associated to $\mathbf{p}$ is

$$W^u(\varepsilon) = \{\mathbf{x} \in \mathbb{R}^n : |\mathbf{F}^k(\mathbf{x}) - \mathbf{p}| < \varepsilon \text{ for all } k \leq 0\}.$$

8.0.2 Remark Both manifolds are invariant to $\mathbf{F}$ by definition.

8.0.3 Theorem ***(Local stable manifold for diffeomorphisms)*** *Let $\mathbf{F} : \mathbb{R}^n \to \mathbb{R}^n$ be a ($\mathcal{C}^1$) diffeomorphism and $\mathbf{p}$ a fixed point. Let $\mathbf{A} = \mathbf{DF}(\mathbf{p})$ have d eigenvalues with absolute value less than 1 and $n-d$ eigenvalues with absolute value greater than 1. Then for ε sufficiently small, $W^s(\varepsilon)$ and $W^u(\varepsilon)$ are smooth manifolds of dimensions d and $n-d$, respectively. If $\mathbf{x} \in W^s(\varepsilon)$ (respectively, $\mathbf{x} \in W^u(\varepsilon)$), then $\mathbf{F}^k(\mathbf{x}) \to \mathbf{p}$ as $k \to +\infty$ (respectively, $\mathbf{F}^k(\mathbf{x}) \to \mathbf{p}$ as $k \to -\infty$). Actually there is a smooth, near indentity change of coordinates that takes the stable and unstable manifolds to (different) coordinate planes.*

8.0.4 Remark As happened in the case of flows, the definition of local stable (or unstable) manifold can be extended to the global case. In order to compute numerically 1-dimensional stable and unstable manifolds for maps we follow the same steps as in the case of flows (see section 4.1).

8.0.5 Remark We already know that each point of a periodic orbit can be seen as a fixed point of the map

$$\mathbf{F} = \phi_T. \tag{8.1}$$

Using this fact for the computation of the stable and unstable manifolds of a PO of the CP problem, we apply that the stable (or the unstable) manifold of a PO contains the manifolds of each point of the orbit, seen as fixed points of (8.1).

The last remark is the key for the numeric computation of the invariant manifolds of PO that we are going to present.

8.1 Invariant manifolds of the LPO around $\mathcal{L}_1$

In this section we are going to take $K = 0.1$. For this value of the parameter, the LPO around $\mathcal{L}_1$ are unstable and, as stated some chapters ago, for $h > h_1 = h_1 = -1.59836975$, the Hill's region of motion has only one component. So we can consider the unstable W^u and stable W^s manifolds associated with them. These invariant manifolds and the existence of homoclinic connections to the Lyapunov orbit are responsible for the dynamics close to the neck around $\mathcal{L}_1$.

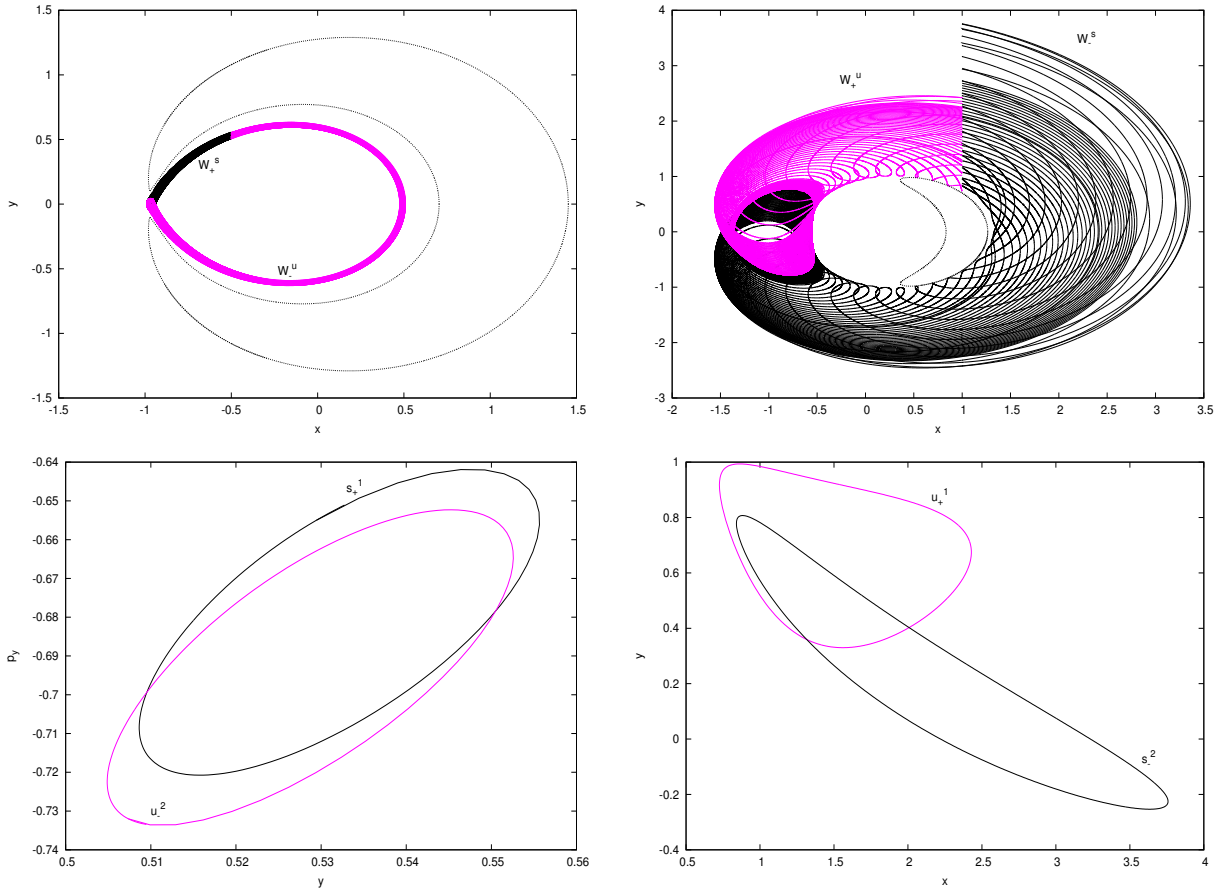

Figure 8.1: $K = 0.1$. The first column of figures has $h = -1.598$ and the second one has $h = -1.464$. Top: the branches of the invariant manifolds associated to a Lyapunov orbit around $\mathcal{L}_1$ in configuration space. The dotted lines represent the zvc at each energy level. Bottom: the sets $u^n_{\mp}$, $s^k_{\pm}$ corresponding to the intersection of the invariant manifolds of the first row with a specific section, plotted in the plane (y, p_y). The intersection points of these sets correspond to homoclinic connections of type $(-2, +1)$ (left) and $(+1, -2)$ (right).

Along this section we take a LPO and $W^{u/s}_{\pm}$ are the branches of the invariant manifolds associated with it (where the sign $\pm$ has the same meaning as in chapter 4). Due to the behaviour of the manifolds, for values of the energy $h > h_1$, close to h_1, the branches $W^{u/s}_{\mp}$ go to the inner region limited by the zero velocity curve around the origin, whereas the branches $W^{u/s}_{\pm}$ go to the outer region, revolving around the zero velocity curve (see the top part of Figure 8.1). Therefore we will find homoclinic connections when the branches $W^{u/s}_{\mp}$ or the branches $W^{u/s}_{\pm}$ intersect. We denote by $u^n_{\pm} = W^u_{\pm} \cap \Sigma^n$ and $s^n_{\pm} = W^s_{\pm} \cap \Sigma^n$ the

intersection of the branches of the invariant manifolds with a given Poincaré section Σ at the n-crossing. We say that there exists a homoclinic orbit of type $(-n,+k)$ if $u^n_- \cap s^k_+ \neq \emptyset$, and of type $(+n,-k)$ if $u^n_+ \cap s^k_- \neq \emptyset$ (see bottom part of Figure 8.1).

8.1.1 Remark In our case, the section considered has been $\Sigma = \{x = a\}$, where a is a fixed and suitable value depending on the energy, the branches taken into account and the value of K.

The branches of the invariant manifolds are 2-dimensional sets, and thus their intersections with a specific section, the sets $u^n_\pm$ and $s^n_\pm$, are 1-dimensional sets. As the energy is constant and the value of the x-coordinate is fixed, we have plotted these intersections in the plane (y, p_y) (see bottom part of Figure 8.1).

The inner homoclinics are obtained when the branches W^u_- and W^s_+ are considered (see left hand side of Figure 8.1). Starting with their second and first intersections respectively with a section $\Sigma = \{x = a\}$, for a constant $a \in [x_1, 0]$, we have found that both branches intersect, for any value of the energy $h > h_1$. Thus there exist at least two families of inner homoclinic connections of type $(-2,+1)$ for a certain range of values of the energy $h > h_1$.

Concerning outer homoclinics, we study the behaviour of the branches W^u_+ and W^s_- up to several intersections with a section Σ. Close to the equilibrium point (i.e., considering LPO with energy close to h_1), these branches do not intersect. As the energy increases, the invariant manifolds get wider and they intersect giving rise to the first outer homoclinics (see right hand side of Figure 8.1). For $h = -1.464$ we have found homoclinics of type $(+1,-2)$.

9 Conclusions

At the beginning of this project we have commented that the aim of this work is to study how to construct a first approach to the dynamics of a given system. For this reason, we decided to study the particular case of the system that models the behaviour of a hydrogen atom in a circularly polarized microwave field, which is a system with a rich dynamics, as we have already seen.

We have dealt with the problem combining two points of view: as a perturbed Kepler problem and as a 2 degree of freedom Hamiltonian problem where the standard tools of Dynamical Systems can be applied.

The thesis has been based on the study of the main invariant objects of the CP problem by means of numerical tools. All the theoretical results and numerical methods needed have been added in order to have a self-contained work. Instead of including the implemented codes in this memory, I have prefered to give the main idea of the implementation of each code.

Combining the obtained results from the different explained invariant objects, we have a first insight of the local and of the global behaviour of the dynamics of our system. Thanks to projects like this one, one can see the importance of the numerical tools, as a support to justify results that analytically could be very difficult.

Bibliography

[1] Esther Barrabés, Mercè Ollé, Florentino Borondo, David Farrelly and Josep M. Mondelo, *Phase space structure of the hydrogen atom in a circularly polarized microwave field*, 2011.

[2] Kenneth R. Meyer, Glen R. Hall, Dan Offin, *Introduction to Hamiltonian Dynamical Systems and the N-Body Problem*, in: Applied Mathematical Sciences, vol. 90, Second edition, Springer, New York, 2009.

[3] Harry Pollard, *Mathematical Introduction to Celestial Mechanics*, Prentice Hall, 1966.

[4] Mercè Ollé, *Class notes from Numerical Methods for Dynamical Systems*, 2014.

[5] Àngel Jorba and Maorong Zou, *Taylor User's Manual*, 2008.

[6] Earl A. Coddington and Norman Levinson, *Theory of ordinary differential equations*, McGraw-Hill, 1972.

[7] Morris W. Hirsch, Robert L. Devaney and Stephen Smale, *Differential Equations, Dynamical Systems and Linear Algebra*, Academic Press, 1974.

[8] E. Barrabés, J.M. Mondelo and M. Ollé, *Dynamical aspects of multi-round horseshoe-shaped homoclinic orbits in the RTBP*, 2009.

[9] Eigen C++ template library for linear algebra: matrices, vectors, numerical solvers, and related algorithms. *Eigen 2 tutorial*, http://eigen.tuxfamily.org/dox-2.0/TutorialCore.html.

[10] Wikipedia, *Apsis*, http://en.wikipedia.org/wiki/Apsis.